Life Sciences 231 (2019) 116527

Contents lists available at ScienceDirect

Life Sciences

journal homepage: www.elsevier.com/locate/lifescie

Proteomic analyses identify a potential mechanism by which extracellular vesicles aggravate ischemic stroke

Xintong Wang[a], Jiaoqi Wang[a], Xiaohua Shi[a], Chengliang Pan[b], Hongyu Liu[a], Yue Dong[a], Rui Dong[a], Jing Mang[a], Zhongxin Xu[a,*]

[a] Department of Neurology, China-Japan Union Hospital, Jilin University, Changchun 130033, Jilin Province, China
[b] College of Clinical Medicine, Jilin University, Changchun, 130021, Jilin Province, China

ARTICLE INFO

Keywords:
Ischemic stroke
Extracellular vesicles
Oxygen glucose deprivation
Oxidative stress
Carbohydrate metabolism

ABSTRACT

Aims: Extracellular vesicles (EVs) are vital for information exchange between donor and recipient cells. When cells are stressed (e.g., by oxygen glucose deprivation, OGD), the complex information carried by the EVs is altered by the donor cells. Here, we aimed to analyze the proteomic differences between EVs derived from OGD-damaged cells and EVs derived from undamaged cells to explore the potential mechanisms by which EVs aggravate ischemic stroke (IS).

Main methods: EVs released by rat adrenal gland PC12 cells subjected to 0, 3, 6, or 12 h of OGD were isolated. The proteins from the EVs secreted by each of the OGD groups were profiled using liquid chromatography-tandem mass spectroscopy (LC-MS/MS). We predicted the functions, pathways, and interactions of the differentially expressed proteins using Gene Ontology (GO), KEGG pathways, and STRING. We used parallel reaction monitoring (PRM) to validate our results.

Key findings: We identified several differentially expressed proteins in the OGD groups as compared to the controls: 170 proteins in the 3 h OGD EVs, 44 proteins in the 6 h OGD EVs, and 77 proteins in the 12 h OGD EVs (fold-change ≥ 1.5; $p \leq 0.05$). These proteins were associated with oxidative stress, carbohydrate metabolism, protein synthesis and degradation, and thrombosis.

Significance: We identified changes in protein expression in the EVs secreted by OGD-damaged cells, highlighting potential mechanisms by which EVs aggravate IS. Our results also suggested potential protein targets, which may be useful for the prevention and treatment of IS.

1. Introduction

Ischemic cerebrovascular disease is one of the main causes of mortality and disability worldwide [1]. Ischemic stroke (IS) is generally triggered by obstructed or restricted blood supplies; decreases in blood supply reduce the flow of oxygen and glucose to the neural cells, and eventually result in neural cell damage or death [1,2]. It is well known that neural cells react differently as the duration of IS increases [3]. The oxygen-glucose deprivation (OGD) model, which mimics the lack of oxygen and glucose during IS, is widely used to explore the injury mechanisms associated with IS [4]. Interestingly, although the intracellular mechanisms of nerve-cell ischemic injury have been extensively investigated [5], it is unclear how damaged cells affect the development of IS. Therefore, exploring the impact of damaged cells on the development of IS can be helpful to further understand the mechanisms by which IS is exacerbated.

Extracellular vesicles (EVs), which are important for cell-cell signal transmission, are lipid bilayer-enclosed extracellular nanovesicles secreted by cells [6]. EVs cross the blood-brain barrier and contain a wide range of functional proteins, lipids, and nucleic acids [6]. EVs have been identified in various types of cells, including neural cells [6–8], and several recent studies have used EVs to treat central nervous system diseases [9–11]. Specifically, it has been shown that EVs derived from mesenchymal stem cells have reparative effects, including neurogenesis and angiogenesis, on tissues damaged by ischemic brain injury [12–14]. Similarly, EVs derived from damaged neural cells cross the blood-brain barrier and affect surrounding neural cells, blood cells, or cells from other organs. However, it is unclear how neural cell damage affects the information carried by the derived EVs, and how this damage subsequently affects IS progression.

In this study, we aimed to determine how the information carried by EVs changed over the course of IS progression, mimicked using the OGD

* Corresponding author.
E-mail address: xuzhongxin9999@163.com (Z. Xu).

https://doi.org/10.1016/j.lfs.2019.06.002
Received 11 April 2019; Received in revised form 20 May 2019; Accepted 1 June 2019
Available online 07 June 2019

model. We also measured the protein content of the EVs, and the effects of OGD EVs on undamaged cells. We used proteomics to investigate these effects, as differences in protein expression among samples (i.e., those with and without OGD damage) allowed us to determine the effects of IS on gene expression [15,16]. Specifically, we used LC-MS/MS to analyze EV protein content, and used Kyoto Encyclopedia of Genes and Genomes (KEGG), Gene Ontology (GO), and Protein-Protein Interaction (PPI) to explore the functional associations of the proteins differently expressed among samples. Parallel reaction monitoring (PRM) absolute quantitation was used to measure changes in the concentrations of target proteins.

2. Materials and methods

2.1. Cell lines and culture

The rat adrenal gland cell line PC12 was purchased from Cell Bank of the Chinese Academy of Sciences (Shanghai, China). PC12 cells were cultured in glucose-free Dulbecco's modified eagle medium (DMEM; GIBCO, Thermo Fisher Scientific, MA, USA), supplemented with 10% fetal bovine serum (FBS), 100 IU/mL streptomycin, and 100 IU/mL penicillin, at 37 °C under humidified air containing 5% CO_2.

2.2. Establishment of the in vitro IS-like OGD model

To induce symptoms of IS in vitro, the cultured PC12 cells were first washed three times with phosphate buffered saline (PBS), and the culture medium was then replaced with glucose-free DMEM, supplemented with 10% EV-depleted FBS (System Biosciences, California, USA). Cells were then placed in a hypoxia chamber (95% N_2 and 5% CO_2) for 3 h, 6 h, or 12 h at 37 °C. Control cells were cultured in high-glucose DMEM (GIBCO, Thermo Fisher Scientific, MA, USA), and then placed in a normoxic (5% CO_2) incubator at 37 °C.

To determine whether the IS model had been successfully established by OGD, apoptosis was detected in the cultured PC12 cells using an Annexin V-FITC PI double staining kit (BD Biosciences, CA, USA), following the manufacturer's instructions. In brief, cells were washed twice with cold PBS and suspended in 1× Binding Buffer to a concentration of 1×10^6 cells/mL. We then transferred 1×10^5 cells to an unused 1.5 mL centrifuge tube and stained the cells with 5 μL Annexin V-FITC and 5 μL PI for 15 min at room temperature in the dark. After staining, the samples were analyzed using a BD Accuri C6 flow cytometer (BD Biosciences, NJ, USA).

2.3. Effects of EVs derived from OGD-damaged cells on undamaged PC12 cells

We used viability assays based on a cell counting kit-8 (CCK-8; Dojindo, Kyushu, Japan) to test the effects of EVs derived from OGD-damaged cells on undamaged PC12 cells. To perform the CCK-8 assays, we first plated 5000 PC12 cells into each well of a 96-well plate. Cells were plated in DMEM medium containing 10% EV-depleted FBS. Cells were treated with either 10 μg or 20 μg of EVs isolated from OGD-damaged cells for 24 h. Cells were then incubated for 2 h with 10 μL CCK-8 per well. Next, the absorbance of each well at 450 nm was measured. Absorbance values were normalized against untreated samples. Assays were performed three times.

2.4. Characterization of the EVs derived from OGD-damaged cells

To obtain EVs from OGD-damaged cells, cultured PC12 cells were washed three times with PBS, and the culture medium was then replaced with glucose-free DMEM and supplemented with 10% EV-depleted FBS. Cells were placed in a hypoxia chamber (95% N_2 and 5% CO_2) for 3 h, 6 h, or 12 h at 37 °C. To obtain control EVs (from undamaged cells), the culture medium was replaced with glucose-free DMEM and supplemented with 10% EV-depleted FBS. Cells were then placed in a normoxic (5% CO_2) incubator at 37 °C. After incubation, the medium was collected. The EVs were isolated and precipitated using the Exosome Precipitation Solution kit (ExoQuick-TC; System Biosciences, California, USA), following the manufacturer's instructions.

We examined the size and form of the EVs in the precipitated pellets using transmission electron microscopy (TEM) to determine whether the EVs obtained from OGD-damaged cells had typical EV membranes (i.e., composed of nanovesicles [6]). The EV pellets were washed three times with PBS, and then suspended in 1 mL PBS. Next, 10 μL aliquots of the EV suspension were added onto 200-mesh formvar-coated grids (Pelco, NY, USA), and each grid was incubated for 10 min at room temperature. Any excess liquid was blotted with filter paper, and then 10 μL 3% phosphotungstic acid were added onto the grid for 5 min at room temperature. Any excess solution was removed with filter paper and the grids were allowed to air dry. Finally, samples were examined and imaged under a TEM (80 kV; JEM-1001, JEOL Ltd., Tokyo, Japan).

Finally, to test specific EV proteins, we performed western blots to detect the EV marker proteins CD63, CD9, CD81, and GAPDH. We ran 10 μg subsamples of each precipitated EV pellet using sodium dodecyl sulfate polyacrylamide gel electrophoresis (SDS-PAGE). Proteins were then transferred to a polyvinylidene fluoride (PVDF) membrane. The membrane was blocked in Tris-Buffered Saline Tween-20 (TBST) containing 5% (*w/v*) non-fat dry milk for 1 h at room temperature. The membrane was incubated with specific anti-CD63, anti-CD9, anti-CD81, and anti-GAPDH primary antibodies (dilution 1:1000; System Biosciences, Palo Alto, California, USA) at 4 °C overnight. The membrane was washed three times with TBST, and incubated with horseradish peroxidase (HRP)-labeled anti-rabbit or anti-mouse secondary antibodies (System Biosciences, Palo Alto, California, USA) for 1 h at room temperature. The membrane was washed in TBST three times, then incubated for 2 min at room temperature with enhanced chemiluminescence (ECL) substrate. Finally, images were captured using Syngene Bio Imaging (Synoptics, Ltd., Cambridge, UK).

2.5. Proteins differentially expressed in OGD EVs

2.5.1. Tandem mass tag (TMT) labeling

We used TMT labeling to identify the proteins differentially expressed between EVs secreted by OGD-damaged cells and EVs secreted by undamaged (control) cells. To extract proteins from the EVs, 100-μg subsamples of each EV pellet were sonicated three times, then centrifuged at 12000 ×*g* to remove debris. Protein concentrations were determined using Bicinchoninic acid (BCA) kits (Beytime, Beijing, China), following the manufacturer's instructions. To digest the proteins, the protein solution was reduced with 5 mM dithiothreitol for 30 min at 56 °C, and alkylated with 11 mM iodoacetamide for 15 min at room temperature in darkness. The urea concentration was maintained at < 2 M by adding 100 Mm triethylamine-carbonic acid buffer (TEAB). Then, trypsin was added to the protein sample at a 1:50 ratio (*w*/w) and allowed to digest overnight. Next, trypsin was added to the protein sample at a 1:100 ratio (w/w) and allowed to digest for 4 h. After trypsin digestion, the resulting peptide was desalted using a Strata X C18 SPE column (Phenomenex, California, USA) and vacuum-dried. The dried peptide was reconstituted in 0.5 M TEAB and labeled using a TMT kit (Thermo Fisher Scientific, MA, USA), following the manufacturer's instructions.

2.5.2. HPLC fractionation

To perform high-pH reverse-phase HPLC fractionation, we transferred the TMT-labeled peptides to Agilent 300Extend C18 columns (particles: 5 μm; internal diameter: 4.6 mm; length: 250 mm; Agilent Technologies Inc., California, USA), and followed the manufacturer's instructions. In brief, we used a fractional gradient of 8–32% acetonitrile (pH 9.0) to separate the peptides into 60 fractions over 60 min. The

peptides were then combined into nine fractions and dried using vacuum centrifugation.

2.5.3. LC-MS/MS analysis

The peptides obtained in section 2.5.2 were dissolved in mobile phase A (0.1% formic acid) and directly loaded onto an EASY-nLC 1000 UPLC system (Thermo Fisher Scientific, MA, USA). Peptides were separated at a constant flow rate of 300 nL/min, using the following liquid gradient: from 0 to 40 min, mobile phase B (0.1% formic acid in 90% acetonitrile) was increased from 6% to 18%; from 40 to 52 min, mobile phase B was increased from 18% to 28%; from 52 to 66 min, mobile phase B was increased from 28% to 80%; and from 66 to 70 min, mobile phase B was held at 80%.

After UPLC separation, peptides were ionized using an NSI ion source (Thermo Fisher Scientific, MA, USA) and analyzed with an Orbitrap Fusion Lumos MS (Thermo Fisher Scientific, MA, USA). The ion source voltage was set to 2.0 kV. We detected and analyzed the peptide precursor and its secondary fragments using high-resolution Orbitrap. The primary MS scan range was 350–1550 *m/z*, at a resolution of 60,000, and the secondary MS scan range had a fixed starting point of 100 *m/z*, at a resolution of 15,000. For data acquisition, we used a data-dependent scanning (DDA) algorithm. That is, only the 20 peptides with the highest signal intensities, as identified by the primary scan, were allowed to enter the HCD collision cell. Then, 32% of the fragmentation energy was used for fragmentation, followed by secondary MS analysis. To increase MS efficacy, the automatic gain control (AGC) was set to 5E4, the signal threshold was set to 5000 ions/s, the maximum injection time was set to 100 ms, and the dynamic exclusion time of the tandem MS scan was set to 30 s (to avoid repeated scans of the parent ions). Proteins were considered differentially expressed between samples if the fold-change was ≥ 1.5 and p was ≤ 0.05. We constructed a Venn diagram, showing the differentially expressed proteins shared and unique among the OGD groups.

2.6. Functional analysis of the proteins differentially expressed among treatment groups

Gene Ontology (GO) annotation is used to express the various attributes of genes and gene products in three major categories: biological processes, cellular composition and molecular functions. To perform GO analysis, we converted the IDs of the identified proteins to UniProt ID using the UniProt database, and then mapped these IDs to GO IDs. To explore the PPIs associated with the differentially expressed proteins, the differentially expressed proteins (Tables 1–3) were imported into the EMBL Search Tool for the Retrieval of Interacting Proteins (STRING) database v 10.5 (http://string.embl.de/) and an interaction map was generated. We next investigated the KEGG pathways associated with the differentially expressed proteins using KEGG online tools.

2.7. Parallel reaction monitoring (PRM)

To validate our TMT and LC-MS/MS results, parallel reaction monitoring (PRM), which quantifies absolute protein concentration, was used to measure the expression of several proteins identified as differentially expressed between the EVs secreted by OGD-damaged cells and the EVs secreted by undamaged (control) cells.

The tryptic peptides were dissolved in 0.1% formic acid and directly loaded onto a reverse-phase analytical column developed in our laboratory. We used an EASY-nLC 1000 UPLC system, with a constant flow rate of 700 nL/min, and the following liquid gradient: from 0 to 38 min, mobile phase B (0.1% formic acid in 98% acetonitrile) as increased from 6% to 23%; from 38 to 52 min, mobile phase B was increased from 23% to 35%; from 52 to 56 min, mobile phase B was increased from 35% to 80%; and from 56 to 60 min, mobile phase B was held at 80%.

The separated peptides were ionized using an NSI source, followed by tandem MS (MS/MS) using a Q ExactiveTM Plus (ThermoFisher Scientific, Bremen, Germany), coupled to the UPLC online. The electrospray voltage applied was 2.0 kV. The *m/z* scan range was 350–1000 for the full scan, and intact peptides were detected in the Orbitrap at a resolution of 35,000. Peptides were selected for MS/MS, with NCE set to 27. Fragments were then detected in the Orbitrap at a resolution of 17,500. We used a data-independent data acquisition procedure, which alternated between one MS scan and 20 MS/MS scans. The AGC was set to 3E6 for full MS scans and 1E5 for MS/MS scans. The maximum IT was set to 20 ms for full MS scans and was automatically set for MS/MS scans. The isolation window for the MS/MS scans was set to 2.0 *m/z*.

We processed the generated MS data using Skyline v.3.6 with the following settings: enzyme set to trypsin [KR/P]; max missed cleavage set to 2; peptide length set to 8–25; variable modifications set to Carbamidomethyl on Cys and oxidation on Met; max variable modifications set to 3; precursor charges set to 2, 3; ion charges set to 1, 2; ion types set to b, y, p; product ions were set to the range ion 3 to the last ion; and the ion match tolerance was set to 0.02 Da. Each PRM assay was performed three times in its entirety.

2.8. Statistical analysis

We determined the statistical significance of differences between group means using paired Student's *t*-tests. We considered values of $p < 0.05$ statistically significant.

3. Results

3.1. OGD induced apoptosis in PC12 cells

To confirm that the OGD model simulated IS in vitro, we subjected PC12 cells to OGD for 3 h, 6 h, or 12 h. Cell viability analysis indicated that the cell death rate increased with OGD duration. The degree of apoptosis, as determined with flow cytometry, was consistent with the cell viability analysis: the apoptotic rate increased with the OGD duration (Fig. 1).

3.2. Characterization of the EVs derived from OGD-damaged PC12 cells

After establishing a stable OGD model, we analyzed the characteristics of EVs derived from OGD-damaged PC12 cells using TEM and western blots. The TEM images showed that the EVs derived from OGD-damaged PC12 cells were bilayer-enclosed nanovesicles with diameters of 30–150 nm. No obvious differences were observed between the control EVs and the EVs exposed to OGD conditions for up to 12 h (Fig. 2A). In addition, the western blots indicated that the expression levels of the EV marker proteins CD63, CD9, CD81, and GAPDH were similar across all groups (Fig. 2B). All EVs, irrespective of OGD duration, expressed the marker proteins.

3.3. EVs derived from OGD-damaged cells induced PC12 cell death

To investigate how the EVs secreted by OGD-damaged cells affected undamaged cells, the EVs derived from OGD damaged cells were co-cultured with undamaged cells for 24 h. The results showed that the EVs derived from OGD-damaged cells had a toxic effect on undamaged cells. The toxic effects of the derived EVs increased with the duration of the OGD experienced by the secreting cell. The average viability of the undamaged cells decreased after treatment with EVs derived from OGD damaged cells (Fig. 3A). The degree of apoptosis indicated by the flow cytometry assay was consistent with the results of the cell viability assay (Fig. 3B).

Table 1
Significantly differentially expressed proteins in the 3 h OGD EVs as compared to the control EVs, as determined with LC-MS/MS (fold-change ≥1.5; p ≤ 0.05).

Protein accession	Protein description	3 h/Ctrl Ratio	Regulated Type	3 h/Ctrl *P* value	Gene name	MW [kDa]	Subcellular localization
F1MAN8	Laminin subunit alpha 5	0.50	Down	2.60E-06	Lama5	4.04E + 02	plasma membrane
Q68FQ0	T-complex protein 1 subunit epsilon	1.84	Up	1.53E-05	Cct5	5.95E + 01	cytoplasm
Q9R1E9	Connective tissue growth factor	0.41	Down	1.53E-05	Ctgf	3.78E + 01	extracellular
Q4FZT9	26S proteasome non-ATPase regulatory subunit 2	1.59	Up	7.68E-05	Psmd2	1.00E + 02	plasma membrane
Q5RKH6	Protein OS-9	0.50	Down	1.83E-04	Os9	7.54E + 01	endoplasmic reticulum
P41562	Isocitrate dehydrogenase [NADP] cytoplasmic	0.42	Down	1.68E-07	Idh1	4.67E + 01	cytoplasm
P30121	Metalloproteinase inhibitor 2	0.55	Down	4.92E-03	Timp2	2.44E + 01	extracellular
P19637	Tissue-type plasminogen activator	0.49	Down	1.39E-04	Plat	6.29E + 01	extracellular
F1LR02	Collagen type XVIII alpha 1 chain	0.65	Down	3.50E-03	Col18a1	1.35E + 02	extracellular
P34901	Syndecan-4	3.00	Up	3.07E-06	Sdc4	2.20E + 01	endoplasmic reticulum
P13832	Myosin regulatory light chain RLC-A	1.88	Up	9.92E-05	Rlc-a	1.99E + 01	mitochondria
G3V6I9	60S ribosomal protein L26	1.82	Up	3.63E-06	Rpl26	1.73E + 01	nucleus
D4A2F1	Agrin	0.59	Down	3.38E-04	Agrn	2.07E + 02	extracellular
B2RYW9	Fumarylacetoacetate hydrolase domain-containing protein 2	0.66	Down	5.36E-03	Fahd2	3.46E + 01	mitochondria
E9PSM5	Matrix metalloproteinase	0.54	Down	1.63E-02	Mmp2	7.42E + 01	extracellular
P84100	60S ribosomal protein L19	2.03	Up	2.60E-04	Rpl19	2.35E + 01	cytoplasm
A0A0A0MXW3	Histone H2A	2.38	Up	3.03E-02	H2afz	1.34E + 01	nucleus
M0RDR2	Uncharacterized protein	0.32	Down	2.60E-04	LOC100909521	6.09E + 01	extracellular
F1 M706	60S ribosomal protein L36	1.62	Up	2.96E-02	LOC100360439	1.23E + 01	nucleus
M0R4G8	TNF alpha-induced protein 6	0.41	Down	3.75E-02	Tnfaip6	3.08E + 01	extracellular
P03994	Hyaluronan and proteoglycan link protein 1	0.66	Down	1.82E-05	Hapln1	4.03E + 01	extracellular
Q6P502	T-complex protein 1 subunit gamma	1.70	Up	1.67E-06	Cct3	6.06E + 01	mitochondria
G3V6X1	Fibulin 2	0.52	Down	2.22E-05	Fbln2	1.31E + 02	extracellular
B5DEH7	C1r protein	0.49	Down	1.30E-03	C1r	8.04E + 01	extracellular
B0BN20	Tetraspanin	0.54	Down	9.67E-05	Tspan6	2.75E + 01	plasma membrane
A9CMB8	DNA helicase	1.54	Up	6.78E-04	Mcm6	9.28E + 01	nucleus
Q642A6	von Willebrand factor A domain-containing protein 1	0.43	Down	2.64E-03	Vwa1	4.48E + 01	extracellular
Q6P6Q5	Amyloid-beta A4 protein	0.59	Down	6.46E-03	App	8.28E + 01	peroxisome
A0A0G2KBA1	Uncharacterized protein	2.40	Up	1.08E-03	–	3.19E + 01	nucleus
G3 V836	Clusterin OS = *Rattus norvegicus* GN = Clu	0.42	Down	1.50E-03	Clu	5.14E + 01	extracellular
F1MA59	Collagen type IV alpha 1 chain GN = Col4a1	0.66	Down	2.08E-03	Col4a1	1.61E + 02	extracellular
A0A0G2JX47	Collagen alpha-1(V) chain	0.57	Down	5.02E-04	Col5a1	1.78E + 02	extracellular
O08628	Procollagen C-endopeptidase enhancer 1	0.55	Down	3.75E-04	Pcolce	5.02E + 01	nucleus
A0A0G2K1L0	Tenascin C	0.45	Down	3.67E-05	Tnc	2.22E + 02	extracellular
A0A0G2JYC6	RCG62582, isoform CRA_c	1.97	Up	3.30E-03	Ubap2l	1.13E + 02	nucleus
Q6IRK8	Spectrin alpha chain, non-erythrocytic 1	1.60	Up	4.16E-06	Sptan1	2.82E + 02	nucleus
G3V7L6	26S proteasome regulatory subunit 7	1.62	Up	1.52E-05	Psmc2	4.86E + 01	cytoplasm
D3ZPK4	Putative uncharacterized protein RGD1565772_predicted	0.60	Down	3.21E-02	Ssc5d	1.52E + 02	extracellular
F1LNH3	Collagen type VI alpha 2 chain	0.42	Down	1.23E-07	Col6a2	1.10E + 02	extracellular
F1 M779	Clathrin heavy chain	1.62	Up	4.77E-07	Cltc	1.92E + 02	cytoplasm
A0A0H2UHQ1	60S ribosomal protein L17	2.16	Up	8.09E-05	Rpl17	2.20E + 01	cytoplasm
G3V7A5	Low density lipoprotein receptor, isoform CRA_a	0.44	Down	8.46E-05	Ldlr	9.66E + 01	plasma membrane
P08082	Clathrin light chain B	1.86	Up	9.19E-04	Cltb	2.51E + 01	cytoplasm,nucleus
P28480	T-complex protein 1 subunit alpha	1.67	Up	3.19E-04	Tcp1	6.04E + 01	cytoplasm
A0A140TAF3	A disintegrin and metalloproteinase with thrombospondin motifs 7	0.47	Down	3.12E-03	Adamts7	1.77E + 02	extracellular
G3V7L3	Complement C1s subcomponent	0.63	Down	4.36E-03	C1s	7.77E + 01	extracellular
A0A0H2UHM3	Haptoglobin	0.64	Down	3.22E-02	Hp	3.84E + 01	extracellular
F1LRA5	Proteoglycan 4	0.54	Down	2.24E-03	Prg4	1.16E + 02	extracellular
D4A6G6	Ribosomal protein S19-like	1.90	Up	2.98E-04	LOC100362339	1.61E + 01	cytoplasm
M0R4L7	Histone H2B	2.11	Up	3.75E-07	Hist1h2bl	1.39E + 01	nucleus
A0A0H2UH99	60S ribosomal protein L24	1.87	Up	1.20E-06	Rpl24	1.77E + 01	cytoplasm
P21531	60S ribosomal protein L3	2.16	Up	1.28E-02	Rpl3	4.61E + 01	cytoplasm
A0A0A0MY14	Ribosomal protein S28-like	1.66	Up	2.54E-02	LOC100359503	7.86E + 00	mitochondria
F1LRL9	Microtubule-associated protein 1B	1.63	Up	6.62E-04	Map1b	2.70E + 02	nucleus
M0RD75	40S ribosomal protein S6	1.72	Up	5.22E-03	Rps6	2.84E + 01	cytoplasm
E9PT66	Splicing factor 3b, subunit 3	1.54	Up	3.34E-02	Sf3b3	1.36E + 02	plasma membrane
E9PTU4	Myosin-11	2.04	Up	1.20E-04	Myh11	2.27E + 02	nucleus
G3V7Z4	Glia-derived nexin	0.47	Down	3.85E-05	Serpine2	4.40E + 01	extracellular
P27615	Lysosome membrane protein 2	1.51	Up	3.96E-02	Scarb2	5.41E + 01	plasma membrane
D3ZUL3	Collagen type VI alpha 1 chain	0.43	Down	2.72E-07	Col6a1	1.09E + 02	extracellular
Q5U362	Annexin	1.63	Up	2.18E-05	Anxa4	3.59E + 01	cytoplasm
P17246	Transforming growth factor beta-1	0.43	Down	1.79E-04	Tgfb1	4.43E + 01	extracellular
Q6PDV7	60S ribosomal protein L10	1.67	Up	1.83E-02	Rpl10	2.46E + 01	cytoplasm
A0A0G2K946	SPARC/osteonectin, cwcv and kazal-like domains proteoglycan 2	0.65	Down	2.48E-05	Spock2	4.70E + 01	extracellular
D3Z9H2	Hyaluronan and proteoglycan link protein 4	0.61	Down	3.97E-02	Hapln4	4.27E + 01	extracellular
D3ZTJ3	ADAM metallopeptidase with thrombospondin type 1 motif, 12	0.42	Down	3.95E-05	Adamts12	1.78E + 02	nucleus
D4AC23	Chaperonin-containing TCP1 subunit 7	1.77	Up	1.67E-05	Cct7	5.97E + 01	cytoplasm
A0A0G2KB28	Predicted gene 6576	1.95	Up	3.97E-04	Gm6576	2.48E + 01	cytoplasm

(*continued on next page*)

Table 1 (*continued*)

Protein accession	Protein description	3 h/Ctrl Ratio	Regulated Type	3 h/Ctrl *P* value	Gene name	MW [kDa]	Subcellular localization
M0R6K0	Laminin subunit beta-2	0.42	Down	4.78E-07	Lamb2	1.97E + 02	extracellular
F1LTJ5	Uncharacterized protein	0.51	Down	4.96E-03	–	2.63E + 02	extracellular
Q6P3V9	60S ribosomal protein L4	2.13	Up	1.40E-03	Rpl4	4.73E + 01	cytoplasm
P04762	Catalase	1.81	Up	6.40E-03	Cat	5.98E + 01	cytoplasm
M0R5K9	Uncharacterized LOC100912024	1.64	Up	5.80E-05	LOC100912024	1.77E + 01	cytoplasm
P16296	Coagulation factor IX	1.73	Up	4.48E-05	F9	5.18E + 01	extracellular
Q5XI84	EGF-containing fibulin extracellular matrix protein 2	0.54	Down	6.11E-05	Efemp2	4.49E + 01	extracellular
D3ZQN7	Laminin subunit beta 1	0.43	Down	5.77E-07	Lamb1	1.97E + 02	extracellular
F1M0X6	Mago homolog B, exon junction complex core component	1.57	Up	9.90E-03	Magohb	1.73E + 01	cytoplasm
G3V9Y1	Myosin, heavy polypeptide 10, non-muscle, isoform CRA_b	1.68	Up	4.27E-08	Myh10	2.29E + 02	cytoplasm
A0A0G2K7W6	Similar to 60S ribosomal protein L27a	1.60	Up	7.96E-04	RGD1562402	1.66E + 01	cytoplasm
D4ACB8	Chaperonin subunit 8 (Theta) (Predicted), isoform CRA_a	1.62	Up	7.80E-05	Cct8	5.96E + 01	cytoplasm
F1MAA7	Laminin subunit gamma 1	0.37	Down	1.97E-08	Lamc1	1.77E + 02	extracellular
F1M6Q3	Collagen type IV alpha 2 chain	0.56	Down	1.81E-04	Col4a2	1.61E + 02	nucleus
D3ZK14	Tenascin N	0.49	Down	6.20E-08	Tnn	1.73E + 02	endoplasmic reticulum
P19139	Casein kinase II subunit alpha	1.61	Up	7.70E-03	Csnk2a1	4.51E + 01	nucleus
R9PXT7	Matrix metalloproteinase	0.59	Down	4.62E-03	Mmp12	5.50E + 01	extracellular
A0A0G2K506	Lactadherin	0.45	Down	1.30E-07	Mfge8	5.11E + 01	extracellular
Q9ERB4	Versican core protein (Fragments)	0.45	Down	1.61E-04	Vcan	3.00E + 02	extracellular
M0RBX6	Histone H3	2.17	Up	1.36E-03	LOC690171	1.54E + 01	nucleus
F1LSW7	60S ribosomal protein L14	2.24	Up	9.16E-04	Rpl14	2.33E + 01	mitochondria
P70560	Collagen alpha-1(XII) chain (Fragment)	0.60	Down	4.57E-04	Col12a1	3.20E + 01	extracellular
Q5XIM9	T-complex protein 1 subunit beta	1.64	Up	3.80E-04	Cct2	5.75E + 01	cytoplasm
Q5RKI5	FLII, actin-remodeling protein	1.57	Up	1.22E-02	Flii	1.45E + 02	cytoplasm
Q499Q4	Phosphoglucomutase 1	0.62	Down	3.71E-05	Pgm1	6.14E + 01	cytoplasm
F1LV50	Collagen and calcium-binding EGF domains 1	0.40	Down	1.37E-04	Ccbe1	3.44E + 01	extracellular
G3V6B1	Transforming growth factor beta-2	0.43	Down	3.34E-08	Tgfb2	5.06E + 01	extracellular
P62718	60S ribosomal protein L18a	2.81	Up	3.98E-04	Rpl18a	2.07E + 01	cytoplasm
Q9QZK5	Serine protease HTRA1	0.58	Down	6.14E-05	Htra1	5.13E + 01	extracellular
A0A0G2K3C8	Nidogen-2	0.45	Down	5.70E-05	Nid2	1.53E + 02	extracellular
P05942	Protein S100-A4	1.53	Up	4.11E-05	S100a4	1.18E + 01	extracellular
P62243	40S ribosomal protein S8	1.83	Up	2.60E-04	Rps8	2.42E + 01	nucleus
D4IGX4	Alpha-(1,6)-fucosyltransferase (Fragment)	0.40	Down	7.99E-04	Fut8	6.65E + 01	endoplasmic reticulum
M0R979	Thrombospondin 1	0.56	Down	2.90E-06	Thbs1	1.27E + 02	nucleus
P62909	40S ribosomal protein S3	1.54	Up	5.70E-05	Rps3	2.67E + 01	cytoplasm
Q1JU68	Eukaryotic translation initiation factor 3 subunit A	1.61	Up	4.42E-04	Eif3a	1.63E + 02	nucleus
Q3KRF2	High density lipoprotein binding protein (Vigilin)	1.81	Up	1.57E-04	Hdlbp	1.42E + 02	cytoplasm
F1LPD0	Collagen alpha-1(XV) chain-like	0.64	Down	2.86E-02	LOC108348074	1.34E + 02	cytoplasm
D4A9N1	HHIP-like 1	0.60	Down	1.70E-02	Hhipl1	8.76E + 01	extracellular
A0A0G2KAJ7	Collagen alpha-1(XII) chain	0.64	Down	3.09E-06	Col12a1	3.43E + 02	extracellular
F1MA79	Slit homolog 2 protein	0.62	Down	5.12E-03	Slit2	1.69E + 02	extracellular
P62250	40S ribosomal protein S16	1.51	Up	1.12E-02	Rps16	1.64E + 01	cytoplasm
G3V6W6	“Proteasome 26S subunit, ATPase 6	1.55	Up	3.82E-04	Psmc6	4.58E + 01	cytoplasm
Q6P9U8	Eukaryotic translation initiation factor 3 subunit H	1.67	Up	4.90E-03	Eif3h	3.99E + 01	cytoplasm
Q63570	26S proteasome regulatory subunit 6B	1.54	Up	2.72E-03	Psmc4	4.74E + 01	cytoplasm
Q642E2	60S ribosomal protein L28	2.17	Up	1.44E-07	Rpl28	1.57E + 01	mitochondria
P11762	Galectin-1	0.60	Down	1.86E-05	Lgals1	1.49E + 01	extracellular
Q06000	Lipoprotein lipase	0.58	Down	1.40E-03	Lpl	5.31E + 01	extracellular
O08727	Tumor necrosis factor receptor superfamily member 11B	0.39	Down	1.57E-06	Tnfrsf11b	4.62E + 01	extracellular
P62804	Histone H4	2.76	Up	8.22E-07	Hist1h4b	1.14E + 01	nucleus
Q66HH8	Annexin	1.72	Up	3.96E-06	Anxa5	3.58E + 01	cytoplasm
D3ZN05	Laminin subunit alpha 3	0.34	Down	1.22E-06	Lama3	1.90E + 02	extracellular
A0A0G2JU77	Eukaryotic translation initiation factor 3 subunit K	1.53	Up	3.14E-03	Eif3k	2.48E + 01	cytoplasm,nucleus
F1LQI4	Aggrecan core protein	0.63	Down	2.19E-02	Acan	2.20E + 02	extracellular
A0A0H2UHL3	Adipocyte enhancer-binding protein 1	0.47	Down	7.54E-05	Aebp1	1.28E + 02	extracellular
Q7TPB1	T-complex protein 1 subunit delta	1.62	Up	1.83E-06	Cct4	5.81E + 01	cytoplasm
Q5RK10	60S ribosomal protein L13a	2.06	Up	1.36E-02	Rpl13a	2.34E + 01	cytoplasm
G3V6P7	Myosin, heavy polypeptide 9, non-muscle	1.86	Up	8.78E-08	Myh9	2.26E + 02	cytoplasm,nucleus
O70513	Galectin-3-binding protein	0.45	Down	6.61E-04	Lgals3bp	6.37E + 01	extracellular
B5DFC8	Eukaryotic translation initiation factor 3 subunit C	1.68	Up	4.38E-04	Eif3c	1.05E + 02	nucleus
F1M6F4	40S ribosomal protein S25-like	1.77	Up	5.23E-04	LOC100912210	1.36E + 01	nucleus
F1LNF0	Myosin heavy chain 14	1.67	Up	6.14E-05	Myh14	2.29E + 02	nucleus
D3ZQ74	Procollagen-lysine, 2-oxoglutarate 5-dioxygenase 1	0.56	Down	1.69E-05	Plod1	8.36E + 01	extracellular
D3ZAF5	Periostin	0.39	Down	1.97E-06	Postn	9.01E + 01	endoplasmic reticulum
B0K031	60S ribosomal protein L7	2.01	Up	2.28E-02	Rpl7	3.03E + 01	cytoplasm
G3V8X6	RCG39455, isoform CRA_a	0.41	Down	1.84E-03	Tsku	3.81E + 01	extracellular
Q63372	Neurexin-1	2.03	Up	1.70E-05	Nrxn1	1.68E + 02	extracellular
G3V9Z6	Septin 8 (Predicted)	1.52	Up	2.54E-02	Sept8	4.99E + 01	cytoplasm
X1WI37	40S ribosomal protein S4	1.56	Up	2.21E-04	Rps4x	2.95E + 01	cytoplasm
B2RZD4	60S ribosomal protein L34	1.90	Up	1.91E-02	Rpl34	1.33E + 01	nucleus

(*continued on next page*)

Table 1 (*continued*)

Protein accession	Protein description	3 h/Ctrl Ratio	Regulated Type	3 h/Ctrl *P* value	Gene name	MW [kDa]	Subcellular localization
Q6P685	Eukaryotic translation initiation factor 2 subunit beta	1.53	Up	3.05E-02	Eif2s2	3.82E + 01	nucleus
F1LT35	Similar to 60S ribosomal protein L23a	1.97	Up	4.42E-03	RGD1564606	1.77E + 01	cytoplasm
F1LND0	Collagen type XVI alpha 1 chain	0.40	Down	1.55E-04	Col16a1	1.59E + 02	cytoplasm
B5DF94	Sushi repeat-containing protein SRPX2	0.40	Down	4.33E-05	Srpx2	5.29E + 01	extracellular
D3ZQ25	Fibulin-1	0.58	Down	1.80E-02	Fbln1	7.81E + 01	extracellular
F1LRT0	Latent-transforming growth factor beta-binding protein 3	0.48	Down	1.54E-06	Ltbp3	1.34E + 02	extracellular
Q6IN14	Tetraspanin	0.52	Down	3.93E-05	Cd82	2.94E + 01	plasma membrane
Q4R1A4	TRK-fused gene protein	2.26	Up	6.58E-04	Tfg	3.10E + 01	cytoplasm
Q3MHS9	Chaperonin containing Tcp1, subunit 6A (Zeta 1)	1.64	Up	1.24E-04	Cct6a	5.80E + 01	cytoplasm
O35142	Coatomer subunit beta	1.56	Up	3.36E-04	Copb2	1.03E + 02	cytoplasm
P49242	40S ribosomal protein S3a	1.81	Up	7.34E-03	Rps3a	2.99E + 01	nucleus
P16409	Myosin light chain 3	1.84	Up	2.57E-07	Myl3	2.22E + 01	cytoplasm
P20961	Plasminogen activator inhibitor 1	0.54	Down	2.22E-04	Serpine1	4.50E + 01	extracellular
F1 M790	Prostaglandin F2 receptor negative regulator	0.53	Down	1.24E-06	Ptgfrn	9.87E + 01	extracellular
D3ZAA3	Latent-transforming growth factor beta-binding protein 1	0.44	Down	3.58E-05	Ltbp1	1.87E + 02	extracellular
Q6IMZ3	Annexin 6	1.60	Up	1.34E-03	Anxa6	7.58E + 01	cytoplasm
D3ZAK6	Ribosomal protein S15, pseudogene 2	1.78	Up	6.88E-03	Rps15-ps2	1.46E + 01	mitochondria
F1LST1	Fibronectin	0.52	Down	1.39E-04	Fn1	2.63E + 02	extracellular
D3ZP82	Lysyl oxidase-like 3	0.54	Down	3.71E-05	Loxl3	8.36E + 01	extracellular
D4AB34	Erythroferrone	0.66	Down	1.04E-02	Erfe	3.64E + 01	extracellular
Q6P9V1	Tetraspanin	0.62	Down	6.17E-05	Cd81	2.59E + 01	plasma membrane
A0A0G2K5E6	60S ribosomal protein L30-like	1.77	Up	1.09E-02	LOC108351936	1.28E + 01	cytoplasm
D3ZD31	Mannose receptor, C type 1	0.64	Down	7.43E-04	Mrc1	1.65E + 02	peroxisome
P04094	Proenkephalin-A	0.56	Down	7.05E-04	Penk	3.09E + 01	extracellular
G3V7G9	"Eukaryotic translation initiation factor 3, subunit 6 interacting protein	1.57	Up	2.44E-03	Eif3l	4.51E + 01	cytoplasm
Q5U328	Nucleolin	1.76	Up	3.22E-03	Ncl	7.73E + 01	nucleus
A0A0G2K6J5	Myosin light polypeptide 6	1.74	Up	8.25E-04	Myl6	1.70E + 01	cytoplasm
A0A0G2JU46	Serine protease 23	0.59	Down	5.04E-03	Prss23	4.41E + 01	extracellular
M0RCH0	Eukaryotic translation initiation factor 3 subunit I	1.57	Up	1.64E-03	Eif3i	3.72E + 01	nucleus
D3Z9E1	Elastin microfibril interfacer 1	0.53	Down	1.76E-03	Emilin1	9.45E + 01	cytoplasm, nucleus
A0A0G2JTT6	HECT and RLD domain-containing E3 ubiquitin protein ligase family member 1	0.27	Down	1.00E-02	Herc1	5.32E + 02	plasma membrane
A0A0G2JWB6	Peroxidasin	0.51	Down	3.89E-05	Pxdn	1.65E + 02	extracellular

3.4. Protein expression in the EVs secreted by OGD-damaged PC12 cells

Compared with traditional protein detection methods, such as western blotting, proteomics-based studies have the ability to systematically and comprehensively elucidate differences in protein composition and expression among different samples. Therefore, TMT labeling and LC-MS/MS were used to investigate the proteomic signatures of the EVs derived from OGD-damaged cells. We identified 1650 distinct proteins across all EV samples; distinct proteins were defined as those with one or more unique peptides. LC-MS/MS analysis identified several proteins significantly differentially expressed in the EVs secreted by the OGD cells as compared to the controls (fold-change ≥ 1.5; $p \leq 0.05$; Fig. 4A): 170 proteins in the 3 h OGD group (Fig. 4A; Table 1); 44 proteins in the 6 h OGD group (Fig. 4A; Table 2), and 77 proteins in the 12 h OGD group (Fig. 4A; Table 3). Venn diagram was used to further analyze the overlap among the differentially expressed proteins in the EVs derived from OGD damaged cells. While 37 differently expressed proteins were shared between the 3 h and 6 h OGD groups (representing 84% of the differentially expressed proteins in the 6 h OGD group), 71 differentially expressed proteins in the OGD 12 h group were unique compared to 3 h and 6 h OGD groups (representing ~92% of the differentially expressed proteins in the 12 h OGD group; Fig. 4B). Only three proteins (SCARB2, LAMA3, and LOC100909521) were shared across the 3 h, 6 h, and 12 h OGD groups (Fig. 4B; Tables 1–3). LOC100909521 is an uncharacterized protein whose predicted gene definition is *Rattus norvegicus* neurosecretory protein VGF-like. There is insufficient understanding of the function of this protein and further research is needed.

GO terms were assigned to the identified proteins based on similarity patterns. Our GO annotations indicated that proteins differentially expressed between the EVs in the OGD groups and the control EVs were primarily associated with cell processes, single biological processes, biological regulation processes, metabolic processes, stimulus response processes, multicellular biological processes, cell development processes and biological origin, localization, and biological adhesion of cell components (biological processes; Fig. 4C); cells, organelles, extracellular matrix, small molecule complexes, and membrane structures (cellular components; Fig. 4D); and binding activity, catalytic activity, structural and molecular activity, and molecular conduction activity (molecular function; Fig. 4E).

In the previous section, we aimed to categorize differences in protein expression, investigate protein function, and quantify differences in target protein expression levels. In this section, we determined the IS-associated regulatory signaling pathways enriched in the differentially expressed proteins. Our cluster analysis indicated that similar KEGG pathways were enriched in the 3 h and 6 h OGD groups. However, the KEGG pathway enriched in the 12 h OGD group differed substantially (Fig. 5). For example, the carbohydrate metabolism, complement and coagulation cascade, ribosome, and lysosome pathways were differently enriched in 3 h, 6 h and 12 h OGD groups (Fig. 5). We then used STRING analysis to systematically analyze the PPIs of GO- and KEGG-identified proteins associated with oxidative stress, carbohydrate metabolism, complement and coagulation, and protein synthesis, folding and degradation (Fig. 6; Supplementary Tables 1–3). Our PPI analysis indicated that the differentially expressed proteins were highly networked, and that information about OGD damage might be transmitted through the interaction network between the differentially expressed proteins in the EVs, thereby damaging the recipient cells (Fig. 6; Supplementary Tables 1–3). Thus, the cell damage caused by continuous OGD may be transmitted via the EVs, leading to recipient cell

Table 2
Significantly differentially expressed proteins in the 6 h OGD EVs as compared to the control EVs, as determined with LC-MS/MS (fold-change ≥1.5; p ≤ 0.05).

Protein accession	Protein description	6 h/Ctrl Ratio	Regulated Type	6 h/Ctrl P value	Gene name	MW [kDa]	Subcellular localization
P41562	Isocitrate dehydrogenase [NADP] cytoplasmic	0.65	Down	1.22E-04	Idh1	46.734	cytoplasm
P34901	Syndecan-4	2.06	Up	2.33E-05	Sdc4	21.962	endoplasmic reticulum
P84100	60S ribosomal protein L19	1.73	Up	6.86E-03	Rpl19	23.466	cytoplasm
A0A0G2K4G5	Fibronectin type III domain-containing protein 1	1.71	Up	6.41E-05	Fndc1	199.64	extracellular
M0RDR2	Uncharacterized protein	0.52	Down	6.24E-04	LOC100909521	60.86	extracellular
A0A0G2KBA1	Uncharacterized protein	1.61	Up	2.48E-03	–	31.926	nucleus
A0A0G2JYC6	RCG62582, isoform CRA_c	1.8	Up	1.18E-03	Ubap2l	112.51	nucleus
A0A0H2UHQ1	60S ribosomal protein L17	1.52	Up	8.00E-04	Rpl17	21.967	cytoplasm
P18291	Granzyme B	1.62	Up	5.87E-05	Gzmb	27.326	extracellular
F1LRA5	Proteoglycan 4	0.57	Down	3.78E-03	Prg4	115.81	extracellular
P21531	60S ribosomal protein L3	1.54	Up	1.81E-02	Rpl3	46.135	cytoplasm
A0A0G2JUA5	AHNAK nucleoprotein	1.53	Up	1.65E-05	Ahnak	581.12	nucleus
P27615	Lysosome membrane protein 2	1.53	Up	2.42E-02	Scarb2	54.09	plasma membrane
Q6PDV7	60S ribosomal protein L10	1.55	Up	2.30E-02	Rpl10	24.604	cytoplasm
D3ZTJ3	ADAM metallopeptidase with thrombospondin type 1 motif, 12	0.62	Down	4.80E-06	Adamts12	178.49	nucleus
A0A0G2KB28	Predicted gene 6576	1.57	Up	1.14E-03	Gm6576	24.793	cytoplasm
M0R6K0	Laminin subunit beta-2	0.64	Down	1.79E-05	Lamb2	196.53	extracellular
Q6P3V9	60S ribosomal protein L4	1.62	Up	4.06E-03	Rpl4	47.3	cytoplasm
D3ZQN7	Laminin subunit beta 1	0.65	Down	1.12E-06	Lamb1	197.39	extracellular
F1MAA7	Laminin subunit gamma 1	0.61	Down	3.57E-07	Lamc1	177.38	extracellular
F1LSW7	60S ribosomal protein L14	1.83	Up	3.18E-03	Rpl14	23.322	mitochondria
Q5RKI5	FLII, actin-remodeling protein	1.76	Up	1.78E-02	Flii	144.86	cytoplasm
P62718	60S ribosomal protein L18a	1.71	Up	4.72E-03	Rpl18a	20.732	cytoplasm
A0A0G2K3C8	Nidogen-2	0.66	Down	4.06E-03	Nid2	152.82	extracellular
Q3KRF2	High density lipoprotein binding protein (Vigilin)	1.59	Up	8.45E-04	Hdlbp	141.69	cytoplasm
Q6P9U8	Eukaryotic translation initiation factor 3 subunit H	1.54	Up	5.40E-04	Eif3h	39.905	cytoplasm
Q642E2	60S ribosomal protein L28	1.77	Up	1.97E-05	Rpl28	15.733	mitochondria
P11762	Galectin-1	0.63	Down	7.74E-05	Lgals1	14.857	extracellular
P62804	Histone H4	1.63	Up	2.63E-06	Hist1h4b	11.367	nucleus
D3ZN05	Laminin subunit alpha 3	0.58	Down	1.94E-06	Lama3	190.08	extracellular
Q5RK10	60S ribosomal protein L13a	1.55	Up	4.38E-02	Rpl13a	23.446	cytoplasm
B5DFC8	Eukaryotic translation initiation factor 3 subunit C	1.63	Up	4.18E-04	Eif3c	105.43	nucleus
Q27W01	RNA-binding protein 8A	0.49	Down	4.12E-05	Rbm8a	19.889	nucleus
D3ZAF5	Periostin	0.66	Down	1.77E-06	Postn	90.055	endoplasmic reticulum
G3V8X6	RCG39455, isoform CRA_a	0.6	Down	2.30E-03	Tsku	38.077	extracellular
G3V9E3	Caldesmon 1, isoform CRA_b	0.64	Down	3.68E-05	Cald1	60.611	nucleus
A0A0G2K273	Eukaryotic translation initiation factor 3 subunit E	1.57	Up	4.48E-03	LOC100909481	52.228	cytoplasm
F1LND0	Collagen type XVI alpha 1 chain	0.63	Down	2.18E-03	Col16a1	159.38	cytoplasm
B5DF94	Sushi repeat-containing protein SRPX2	0.59	Down	4.11E-05	Srpx2	52.852	extracellular
Q4R1A4	TRK-fused gene protein	1.98	Up	1.20E-03	Tfg	31.025	cytoplasm
O35142	Coatomer subunit beta	1.55	Up	1.81E-04	Copb2	102.55	cytoplasm
D3ZGL3	Hedgehog-interacting protein	1.53	Up	6.43E-04	Hhip	78.582	extracellular
P04094	Proenkephalin-A	0.65	Down	2.31E-05	Penk	30.932	extracellular
A0A0G2JTT6	HECT and RLD domain-containing E3 ubiquitin protein ligase family member 1	0.51	Down	4.38E-04	Herc1	531.54	plasma membrane

dysfunction or death, and aggravating disease progression.

3.5. PRM validation

To validate the MS data generated by the TMT analysis, we used PRM, which quantifies absolute protein concentration, to measure the expression of several proteins identified as differentially expressed between the EVs secreted by OGD-damaged cells and the EVs secreted by undamaged (control) cells. We selected seven of the proteins recovered as differentially expressed by the TMT analysis for PRM validation: CAT, IDH1, PGM1, PSMC2, TCP1, PLAT, and MFGE8. Abnormalities in the expression levels of these proteins are related to carbohydrate metabolism, oxidative stress, protein synthesis and degradation, thrombosis, and angiogenesis. In general, there was good agreement between the MS and PRM analyses for the seven selected proteins (Fig. 7; Fig. S1). That is, the PRM analysis identified all seven proteins as differentially expressed between the EVs derived from OGD-damaged cells and the control EVs.

4. Discussion

EVs, as messengers of intercellular signal transduction, play important regulatory roles in disease development, progression, diagnosis, and treatment [17,18]. IS, which is a neurological disease with high fatality and disability rates, seriously endangers human life and health [1]. EVs provide a new strategy for the treatment of ischemic stroke. Most previous studies have shown that stem cell-derived EVs have obvious curative effects on IS [19,20]. However, studies of the effects of EVs derived from nerve cells damaged by IS on disease progression are relatively rare. Several in vitro models that simulate IS are available, including chemical, enzymatic, and OGD methods [21]. Of these, OGD is the most reproducible and produces the best results [21]. Therefore, we simulated IS using the PC12 cell OGD model, and explored the protein composition and functionality of EVs derived from damaged cells (Fig. 1). Our results indicated that cell apoptosis increased significantly with OGD duration. The EVs secreted by damaged cells were typical in form and size and expressed EV marker proteins (CD63, CD9, CD81, and GAPHD; Fig. 2). Further functional analyses showed that OGD-derived EVs induced apoptosis in undamaged cells, and the that

Table 3
Significantly differentially expressed proteins in the 12 h OGD EVs as compared to the control EVs, as determined with LC-MS/MS (fold-change ≥1.5; p ≤ 0.05).

Protein accession	Protein description	12 h/Ctrl Ratio	Regulated Type	12 h/Ctrl P value	Gene name	MW [kDa]	Subcellular localization
A0A0G2K3Q6	Fructose-bisphosphate aldolase	1.86	Up	1.28E-02	Aldoc	40.484	cytoplasm
A0A0G2K890	Ezrin	1.57	Up	9.57E-04	Ezr	69.287	cytoplasm
Q6AXR4	Beta-hexosaminidase subunit beta	2.09	Up	8.83E-04	Hexb	61.527	mitochondria
Q63198	Contactin-1	2.91	Up	2.68E-02	Cntn1	113.49	peroxisome
A0A0G2K8T0	Acid ceramidase	1.82	Up	2.18E-04	Asah1	48.282	mitochondria
Q4V7D1	Signal sequence receptor, alpha	1.63	Up	2.46E-03	Ssr1	32.207	endoplasmic reticulum
P12843	Insulin-like growth factor-binding protein 2	2.42	Up	5.96E-05	Igfbp2	32.854	extracellular
Q5PPG5	Chga protein	0.53	Down	5.64E-05	Chga	51.896	extracellular
F1LPC7	Hepatoma-derived growth factor	0.59	Down	3.65E-05	Hdgf	26.44	nucleus
F7FJQ3	NPC intracellular cholesterol transporter 2	2.18	Up	4.10E-05	Npc2	16.748	extracellular
G3 V803	Cadherin-2	2.63	Up	5.92E-03	Cdh2	99.667	peroxisome
Q6PDW4	Proteasome subunit beta type	1.7	Up	2.18E-05	Psmb1	26.407	cytoplasm,nucleus
P14630	Apolipoprotein M	1.54	Up	1.27E-06	Apom	21.512	extracellular
M0RDR2	Uncharacterized protein	0.54	Down	7.42E-04	LOC100909521	60.86	extracellular
F1LUV9	Neural cell adhesion molecule 1	1.84	Up	6.06E-03	Ncam1	91.635	cytoplasm
Q5XI73	Rho GDP-dissociation inhibitor 1	1.69	Up	1.70E-05	Arhgdia	23.407	cytoplasm
P31399	ATP synthase subunit d, mitochondrial	1.65	Up	1.61E-04	Atp5h	18.763	cytoplasm
A0A1B0GWM3	Laminin subunit alpha 3 (Fragment)	0.66	Down	6.26E-05	Lama3	230.89	cytoplasm
Q6AYK6	Calcyclin-binding protein	0.65	Down	3.20E-04	Cacybp	26.541	nucleus
A0A0G2K7E5	Voltage-dependent calcium channel subunit alpha-2/delta-1	1.65	Up	1.69E-02	Cacna2d1	122.73	extracellular
G3V8U9	Proteasome subunit beta	1.56	Up	5.54E-03	Psmb4	25.76	cytoplasm,nucleus
R9PXU6	Vinculin	2.38	Up	4.35E-07	Vcl	116.57	cytoplasm
P00507	Aspartate aminotransferase, mitochondrial	1.58	Up	1.15E-04	Got2	47.314	mitochondria
Q9EPB1	Dipeptidyl peptidase 2	2.66	Up	3.65E-05	Dpp7	55.114	plasma membrane
P29534	Vascular cell adhesion protein 1	2.07	Up	1.78E-04	Vcam1	81.245	plasma membrane
Q05982	Nucleoside diphosphate kinase A	1.79	Up	1.72E-05	Nme1	17.193	cytoplasm
D3ZS25	Similar to High mobility group protein 2 (HMG-2)	0.59	Down	1.28E-03	RGD1561694	23.997	nucleus
Q6P6T6	Cathepsin D	1.75	Up	9.85E-04	Ctsd	44.622	extracellular
Q5FVS2	Kallikrein B, plasma 1	1.96	Up	1.90E-03	Klkb1	71.282	extracellular
F1LQP8	Cadherin-6	3.53	Up	3.97E-07	Cdh6	88.449	mitochondria
G3 V824	Insulin-like growth factor 2 receptor	1.66	Up	2.12E-05	Igf2r	273.59	extracellular,plasma membrane
P27615	Lysosome membrane protein 2	1.73	Up	1.50E-02	Scarb2	54.09	plasma membrane
G3 V741	Phosphate carrier protein, mitochondrial	1.53	Up	5.65E-04	Slc25a3	39.531	nucleus
D3ZHG3	Protein tyrosine kinase 7	1.64	Up	3.85E-02	Ptk7	86.263	mitochondria
G3V8G9	Neurogenic locus notch homolog protein 2	1.61	Up	1.59E-05	Notch2	265.13	extracellular,plasma membrane
P32551	Cytochrome b-c1 complex subunit 2, mitochondrial	1.51	Up	3.66E-02	Uqcrc2	48.396	mitochondria
Q9JHW0	Proteasome subunit beta type-7	1.52	Up	1.10E-03	Psmb7	29.927	cytoplasm
Q5EBA7	HGF activator	1.53	Up	2.78E-04	Hgfac	70.736	extracellular
F7EQ81	*N*-acetylglucosamine-6-sulfatase	1.94	Up	3.36E-03	Gns	55.413	cytoplasm
P20909	Collagen alpha-1(XI) chain	1.68	Up	2.43E-04	Col11a1	181.02	mitochondria
D3ZBS2	Inter-alpha-trypsin inhibitor heavy chain H3	2.33	Up	1.72E-03	Itih3	99.066	endoplasmic reticulum
A0A0G2K1S6	Malic enzyme	2.57	Up	1.33E-07	Me1	63.832	nucleus
B2RZ96	LOC689226 protein	0.66	Down	1.56E-02	Ube2r2	27.166	cytoplasm,nucleus
A0A0G2K0V8	Nuclear migration protein nudC-like	0.65	Down	1.72E-05	LOC100911422	32.4	nucleus
R9PXT7	Matrix metalloproteinase	1.52	Up	4.52E-03	Mmp12	54.987	extracellular
F1LMH7	Fibroblast activation protein, alpha	1.97	Up	3.50E-05	Fap	87.714	endoplasmic reticulum
F7EPE0	Prosaposin	1.63	Up	1.62E-05	Psap	61.453	extracellular
P29419	ATP synthase subunit e, mitochondrial	1.54	Up	1.05E-02	Atp5i	8.2545	cytoplasm
F1LRA1	Protein ERGIC-53	1.59	Up	1.28E-03	Lman1	57.985	Golgi apparatus
F7FMS0	Macrophage-stimulating 1	1.71	Up	3.55E-05	Mst1	83.144	extracellular
P06214	Delta-aminolevulinic acid dehydratase	2.94	Up	3.72E-05	Alad	36.031	mitochondria
Q5XI38	Lymphocyte cytosolic protein 1	1.95	Up	8.31E-05	Lcp1	70.121	cytoplasm
P40307	Proteasome subunit beta type-2	1.51	Up	8.64E-04	Psmb2	22.912	cytoplasm
A0A0G2QC21	Rho guanine nucleotide exchange factor 7	1.54	Up	6.56E-03	Arhgef7	97.165	nucleus
A0JPM9	Eukaryotic translation initiation factor 3 subunit J	0.61	Down	3.00E-02	Eif3j	29.187	nucleus
B5DFD6	Tie1 protein	3.04	Up	4.55E-06	Tie1	125.21	extracellular
Q27W01	RNA-binding protein 8A	0.44	Down	7.63E-05	Rbm8a	19.889	nucleus
F1 M305	ABI family member 3-binding protein	1.77	Up	1.42E-03	Abi3bp	94.546	mitochondria
Q63083	Nucleobindin-1	2.52	Up	4.04E-03	Nucb1	53.506	extracellular
Q6IN37	GM2 ganglioside activator	2.17	Up	7.55E-05	Gm2a	21.493	extracellular
Q6P762	Alpha-mannosidase	1.75	Up	2.58E-04	Man2b1	114.33	nucleus
F1MAH6	Cadherin 11	3.3	Up	6.03E-04	Cdh11	88.035	endoplasmic reticulum
D3Z8I7	“Glutathione S-transferase, theta 3	1.66	Up	1.83E-02	Gstt3	23.381	extracellular
P05065	Fructose-bisphosphate aldolase A	2.03	Up	1.78E-05	Aldoa	39.351	cytoplasm
P20961	Plasminogen activator inhibitor 1	2.01	Up	1.89E-05	Serpine1	45.009	extracellular
F1M7X3	Cadherin 13	2.19	Up	6.24E-03	Cdh13	66.473	cytoplasm
Q6P503	ATPase H + -transporting V1 subunit D	1.69	Up	1.33E-02	Atp6v1d	28.309	cytoplasm

(*continued on next page*)

Table 3 (*continued*)

Protein accession	Protein description	12 h/Ctrl Ratio	Regulated Type	12 h/Ctrl P value	Gene name	MW [kDa]	Subcellular localization
O88989	Malate dehydrogenase, cytoplasmic	1.55	Up	2.14E-02	Mdh1	36.483	cytoplasm
P97603	Neogenin (Fragment)	2.71	Up	1.80E-07	Neo1	150.64	plasma membrane
Q641X3	Beta-hexosaminidase subunit alpha	2.08	Up	1.78E-04	Hexa	60.537	extracellular
G3V7X5	SPARC-like 1 (Mast9, hevin), isoform CRA_a	0.63	Down	1.74E-02	Sparcl1	70.553	extracellular
O35276	Neuropilin-2	1.72	Up	3.28E-03	Nrp2	103.9	peroxisome
M0R6E6	Scaffold attachment factor B2	0.65	Down	1.66E-02	Safb2	89.964	nucleus
Q499S6	Cathepsin F	1.91	Up	3.59E-02	Ctsf	51.829	extracellular
Q64610	Ectonucleotide pyrophosphatase/ phosphodiesterase family member 2	2.65	Up	3.28E-03	Enpp2	101.58	extracellular
A0A0G2JTA6	Insulin-like growth factor 2, isoform CRA_b	1.59	Up	7.68E-05	Igf2	21.117	extracellular
Q6IN22	Cathepsin B	1.64	Up	1.60E-02	Ctsb	37.544	extracellular

effects of the damaged EVs on recipient cells increased with OGD treatment duration (Fig. 3).

Here, we identified some proteins significantly differentially expressed in EVs derived from OGD-damaged cells, as compared to those derived from undamaged cells (Fig. 4A). The EVs secreted by cells subjected to shorter durations of OGD (3 h and 6 h) shared many differentially expressed proteins (Fig. 4B). However, many of the proteins differentially expressed in the 12 h OGD EVs were unique (Fig. 4B). The GO results were divided into three categories: biological processes, cellular components, and molecular functions (details of the differently expressed proteins in each group are shown in Fig. 4C-E). There were both similarities and differences among the treatment groups with respect to the three GO categories. This suggested that cells might remain relatively stable when subjected to up to 6 h of OGD, but that cell properties might change substantially if the OGD duration was increased to 12 h. Clinical guidelines state that IS should optimally be treated within 4.5 h, but that this period can be extended to 6 h [22,23]. Our results are roughly consistent with ischemic brain injury clinical guidelines.

We investigated the PPIs of the differentially expressed proteins associated with oxidative stress, carbohydrate metabolism, and complement and coagulation in the damaged cell-derived EVs (Fig. 6). The results showed that the differentially expressed proteins formed a complete functional interaction network. This network transferred complicated information from the donor cells to the recipient cells, and thus had regulatory effects on the recipient cells (Fig. 6). We validated seven differently expressed proteins closely related to IS (CAT, IDH1, PGM1, PSMC2, TCP1, PlAT, and MFGE8) using PRM quantification, and closely analyzed their specific effects (Fig. 7). These proteins are associated with oxidative stress, carbohydrate metabolism, complement and

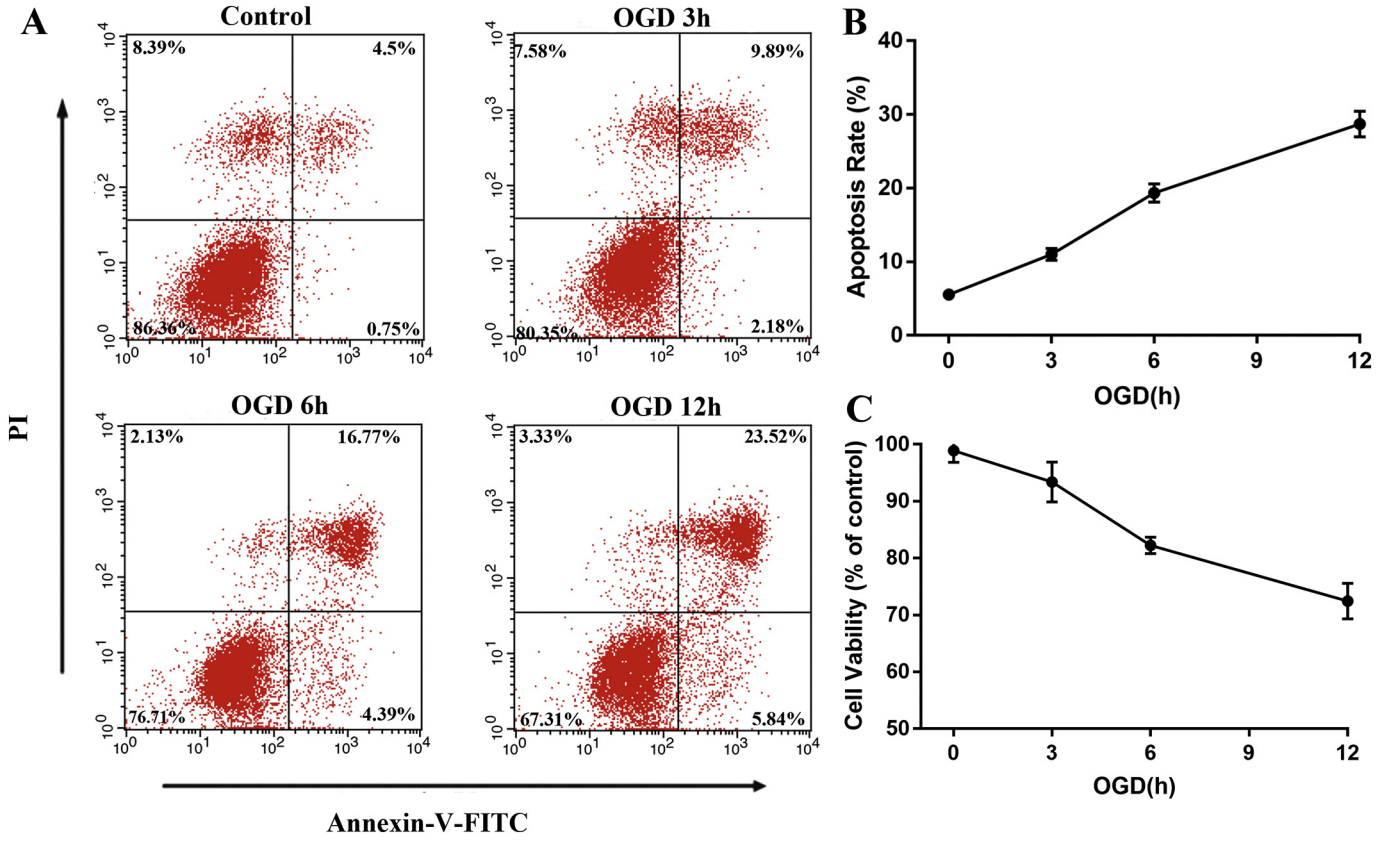

Fig. 1. Oxygen glucose deprivation (OGD) induces apoptosis in PC12 cells. (A) Apoptosis rate in PC12 cells subjected to OGD for 0 h (control), 3 h, 6 h, or 12 h, as measured using flow cytometry. (B) Apoptosis rate in PC12 cells subjected to OGD for 0 h (control), 3 h, 6 h, or 12 h, as measured using flow cytometry. Each point represents the means ± standard deviation of three replicates. (C) Cell viability rate in PC12 cells subjected to OGD for 0 h (control), 3 h, 6 h, or 12 h, as measured with a CCK-8 assay. Each point represents the means ± standard deviation of three replicates.

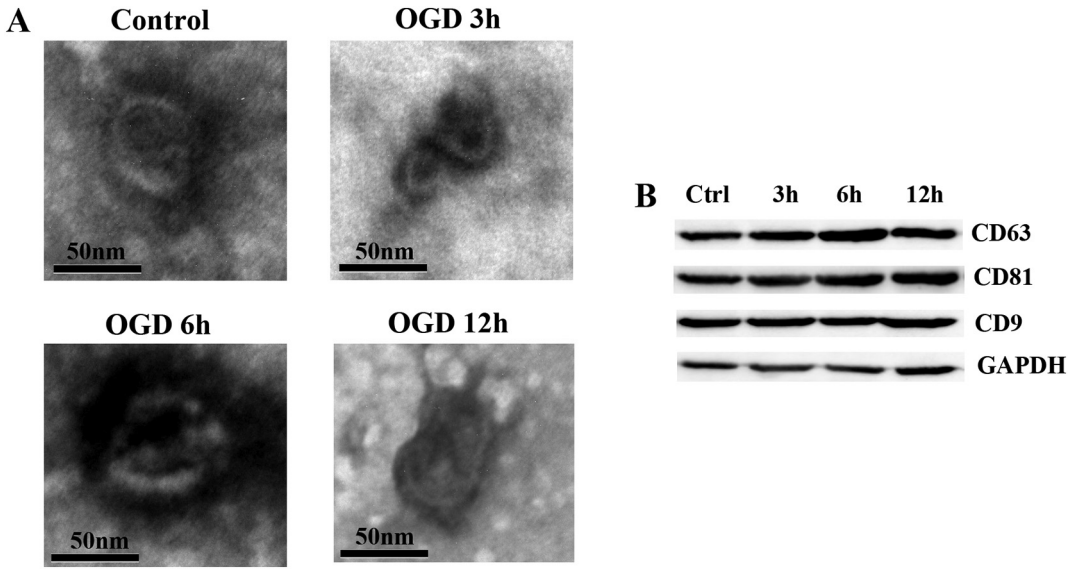

Fig. 2. Characterization of the extracellular vesicles (EVs) isolated from PC12 cells subjected to OGD for 0 h (control), 3 h, 6 h, or 12 h. (A) Transmission electronic micrographs of EVs in different treatment groups. Note that the EVs are of similar size and shape across all groups. (B) Western blot showing that the expression levels of four EV marker proteins (CD63, CD9, CD81, and GAPDH) were similar across treatment groups.

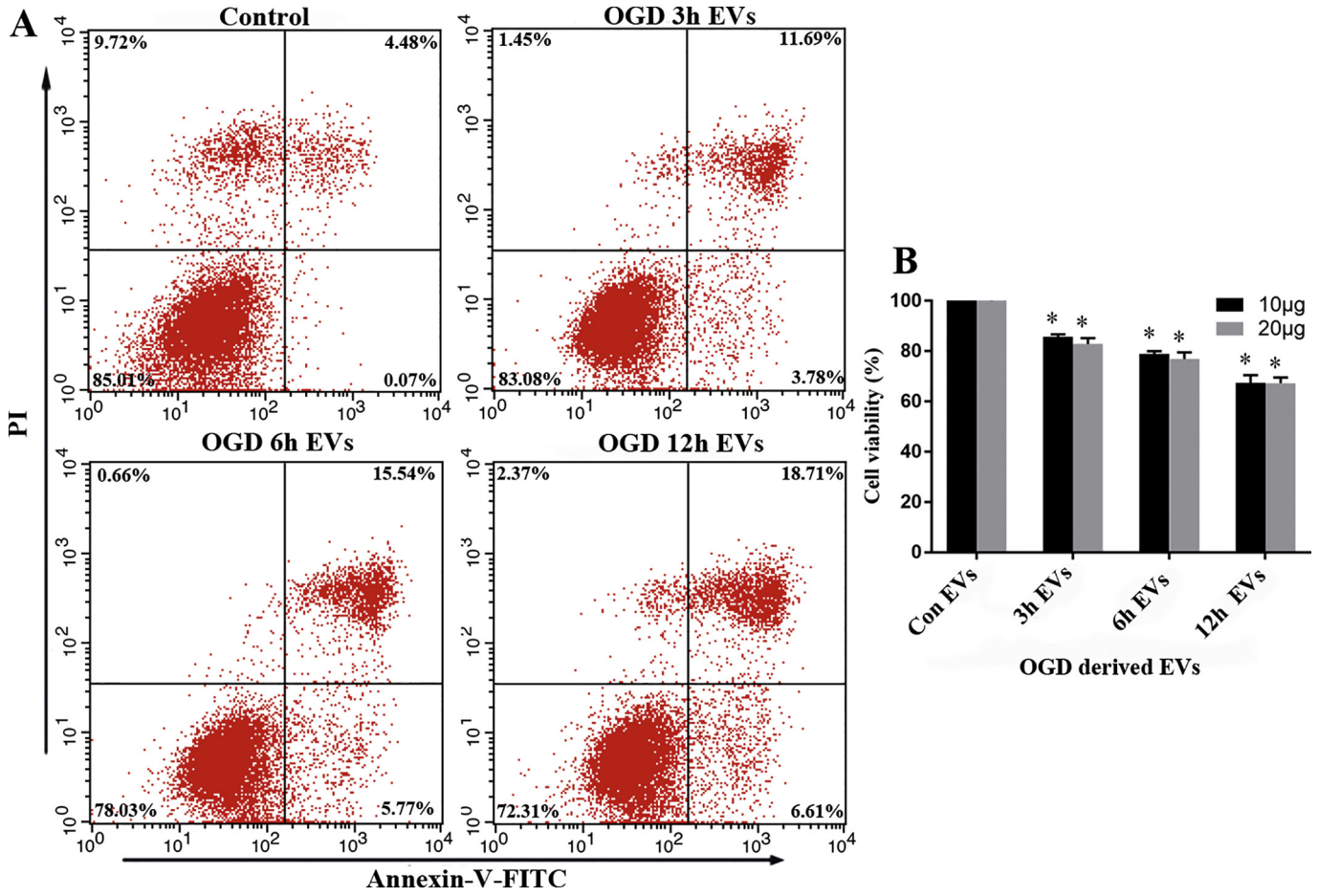

Fig. 3. Apoptosis and viability of undamaged cells after treatment with extracellular vesicles (EVs) isolated from OGD-damaged PC12 cells. EVs were isolated from PC12 cells subjected to OGD for 0 h (control), 3 h, 6 h, or 12 h, then co-cultured with undamaged cells for 24 h. (A) Apoptosis rate, as measured with flow cytometry. Undamaged cells were treated with 10 μg of EVs derived from damaged cells. (B) Cell viability rate, as measured with a CCK-8 assay. Values were normalized against untreated samples. Bars indicate the means of three independent measurements; error bars indicate standard deviation. * indicates $p \leq 0.05$ compared with control.

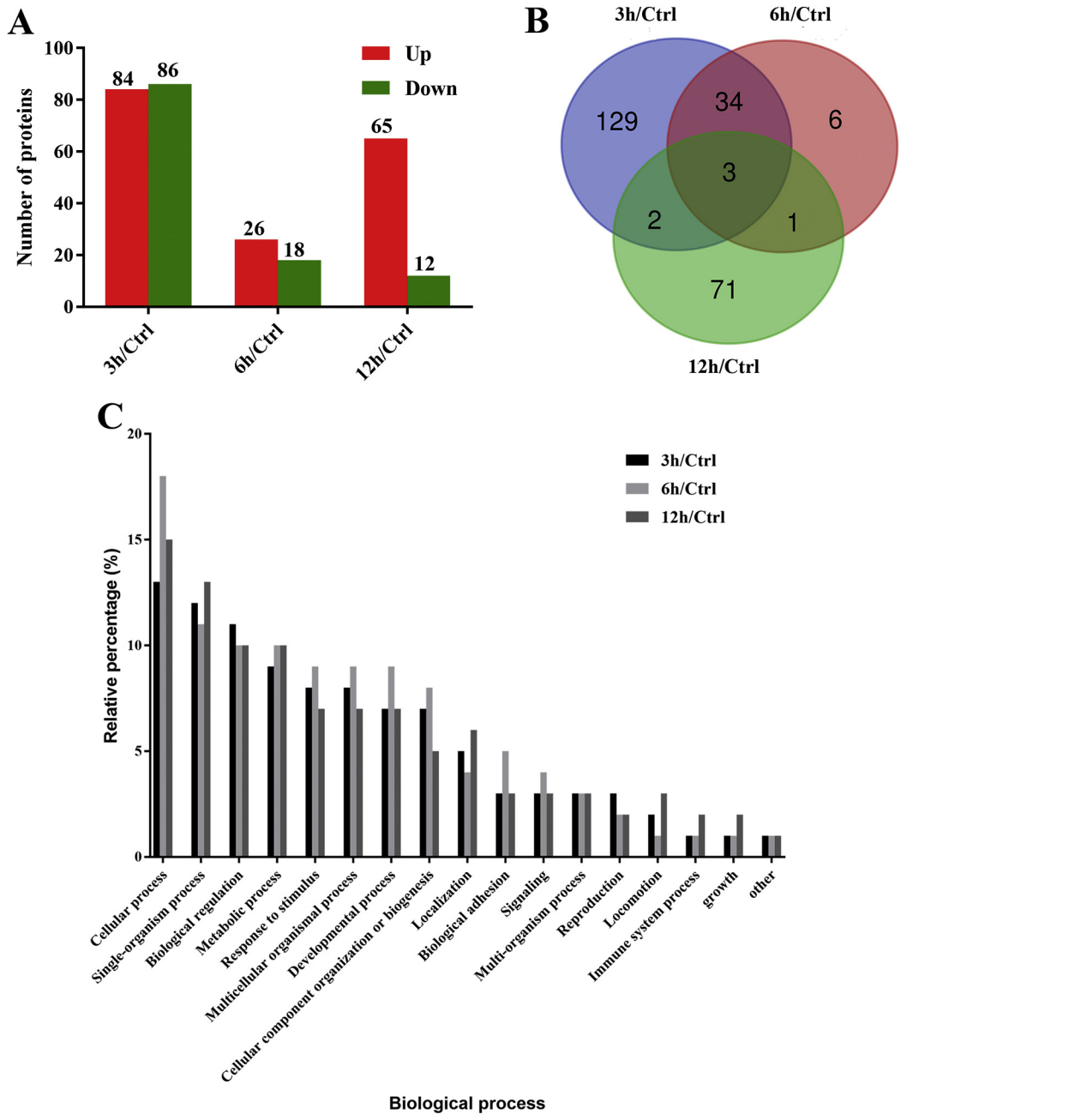

(caption on next page)

Fig. 4. Characterization of the proteins from extracellular vesicles (EVs) isolated from PC12 cells subjected to OGD for 0 h (control), 3 h, 6 h, or 12 h. (A) Proteins significantly differentially expressed between the OGD EVs and the control EVs. (B) Venn diagram showing the overlap in differently expressed proteins among the EV OGD groups. (C–E) Gene ontology of the differentially expressed proteins in the OGD EVs as compared to control EVs in (C) biological processes, (D) cellular components, and (E) molecular function; the vertical axis represents the number of differentially expressed proteins associated with each functional category as a percentage of all differentially expressed proteins.

coagulation, protein synthesis and degradation, and angiogenesis. The characterization of these proteins might help us to understand how EVs derived from cells damaged by IS affect the recipient cells and disease progression.

During ischemic brain injury, some brain tissues become hypoxic due to insufficient blood supply; this induces oxidative stress [24]. The primary function of CAT is to hydrolyze hydrogen peroxide, preventing peroxide damage to cells. Here, CAT expression levels were the highest in the 3 h OGD group (twice as high as the control group). As OGD duration increased, CAT expression levels in the EVs decreased. CAT expression levels in the EVs in the 12 h OGD group were similar to those of the EVs in the control group. These results suggested that, in the initial stage of OGD, cells increase their resistance to ROS damage by increasing CAT expression [25]. As OGD is prolonged, the resistance of the cell to antioxidant stress gradually weakens, and the increase in ROS triggers further cell damage and even death [26]. EVs transmit

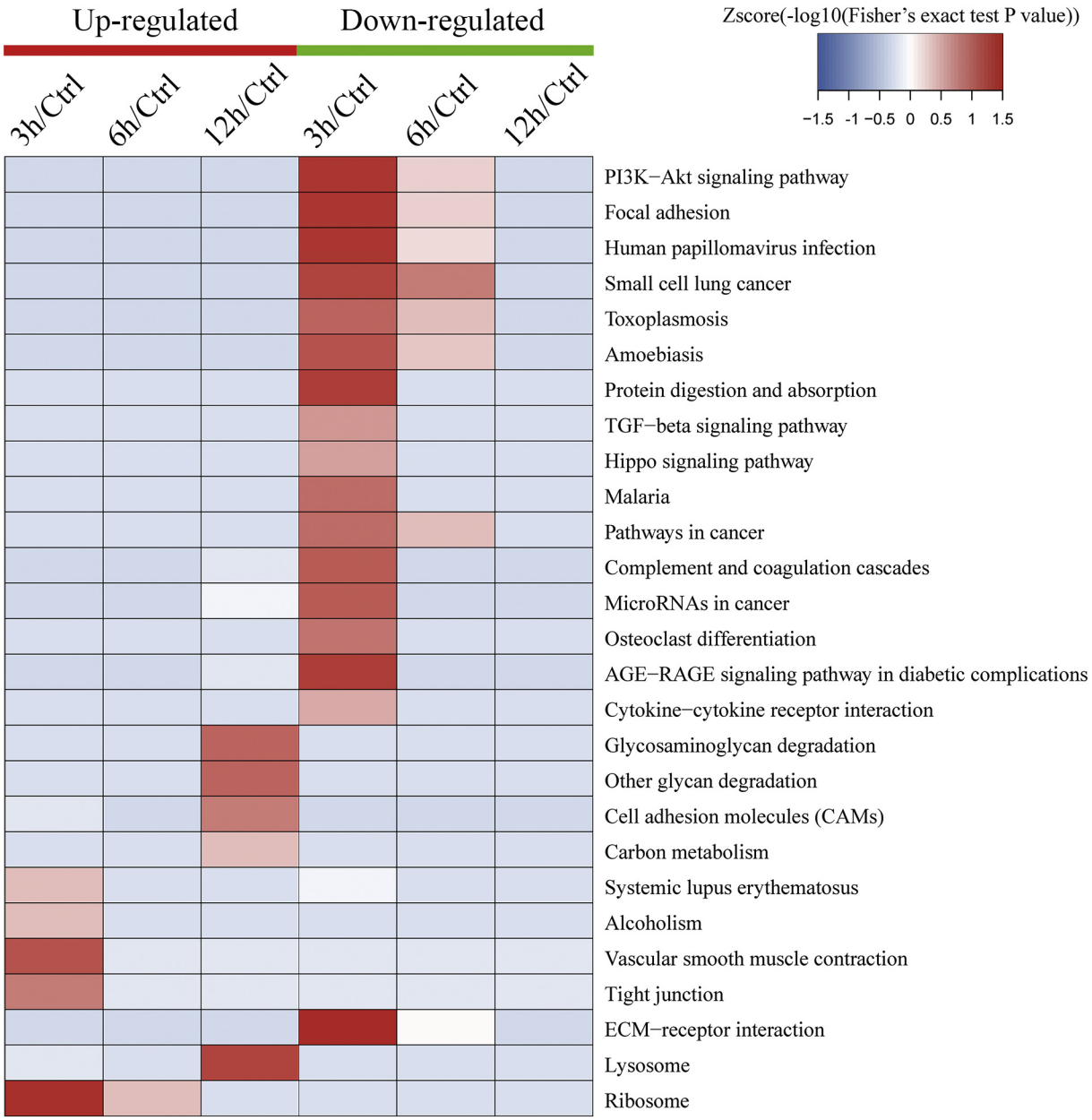

Fig. 5. KEGG pathway cluster analysis of the proteins differentially expressed in the EVs isolated from OGD cells. The enrichment analysis uses a hierarchical clustering method based on Fisher's exact test to group related functions together and draws these clusters as heatmap. The rows of the heat map represent the enrichment of different treatment groups, and the columns represent the enrichment of different KEGG pathways, with color corresponding to the degree of enrichment: red indicates strong enrichment and blue indicates weak enrichment. (For interpretation of the references to color in this figure legend, the reader is referred to the web version of this article.)

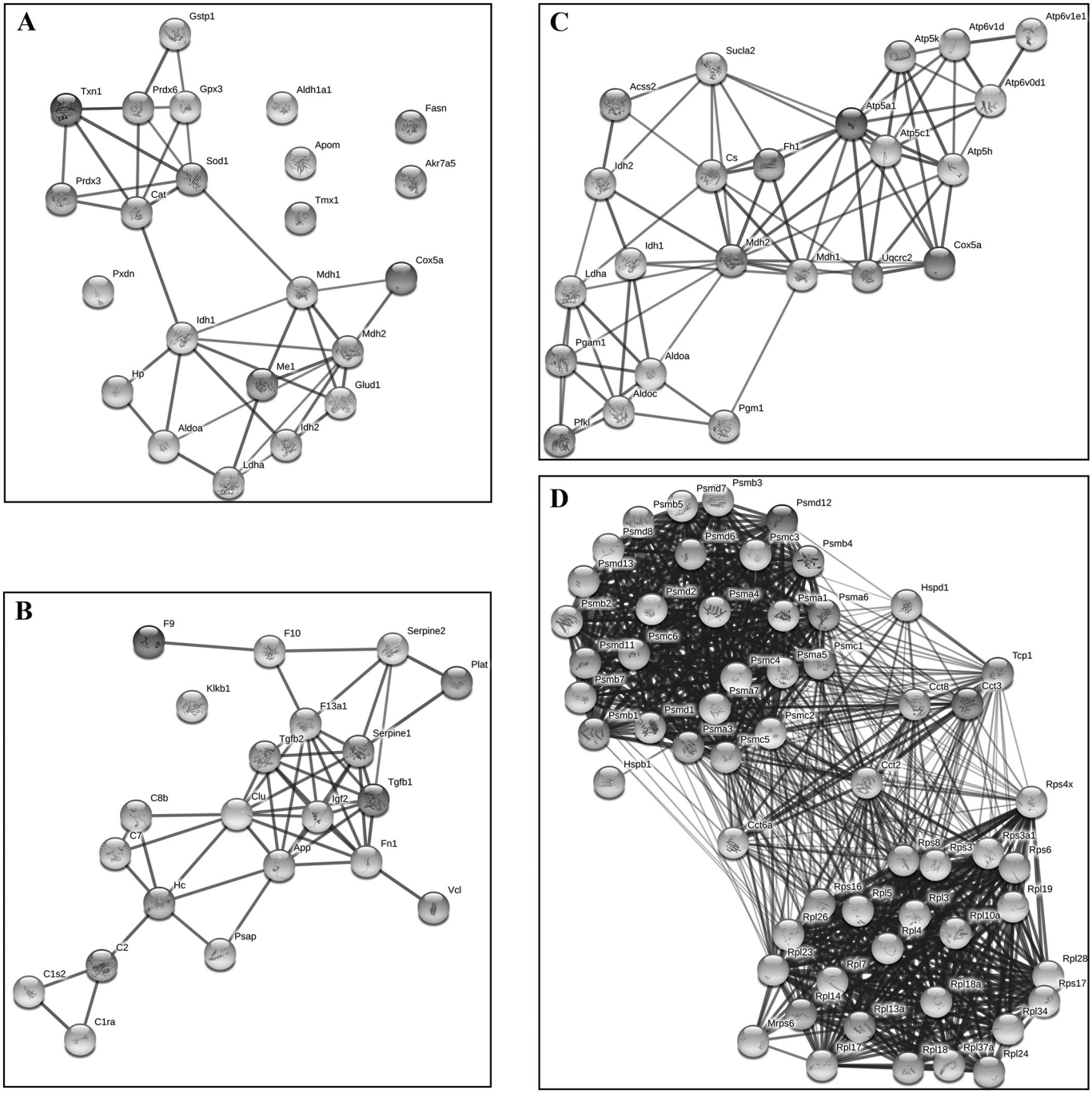

Fig. 6. Protein-protein interaction networks for the proteins differentially expressed (fold-change ≥ 1.2; p ≤ 0.05) in the extracellular vesicles (EVs) isolated from PC12 cells subjected to OGD. (A) Proteins associated with oxidative stress. (B) Proteins associated with complement and coagulation. (C) Proteins associated with the carbohydrate metabolism. (D) Proteins associated with protein synthesis, folding, and degradation. Each node represents a protein. Colored nodes represent the queried proteins and the first level of interaction. Filled nodes represent proteins with known or predicted 3-dimensional (3D) structures; empty nodes proteins with unknown 3D structures. Interactions (edges) were generated based on experimental data, text-mining, co-expression, co-occurrence, gene fusion, and database information. Only high confidence interactions are shown (minimum interaction score = 0.07), with thicker lines representing higher confidence interactions.

oxidative stress information from donor cells to recipient cells, thereby inducing oxidative stress in the recipient cells.

Under normal conditions, cells produce ATP via tricarboxylic acid cycling and oxidative phosphorylation. In addition to oxidative stress, IS also causes abnormalities in energy metabolisms, accompanied by carbohydrate metabolism dysfunction. PGM1, which is critical for carbohydrate metabolism, catalyzes the bidirectional conversion between G-1-P and G-6-P. The conversion of G-1-P to G-6-P generates a key intermediate for cell glycolysis, while the conversion of G-6-P to G-1-P provides UDP-glucose for cellular synthesis of non-essential components [27]. Therefore, PGM1 is important for the regulation of carbohydrate metabolism. Our results indicated that PGM1 was down-regulated in the EVs derived from OGD-damaged cells as compared to the controls (Fig. 7). IDH1 catalyzes the conversion of citric acid to alpha-ketoglutarate, as well as the conversion of NAD+ to NADH. These processes generate essential substrates for the tricarboxylic acid cycle (TAC), completing the transfer of electron links [28]. Since IDH1 is the rate-limiting enzyme of the TAC, it plays an important role in cell

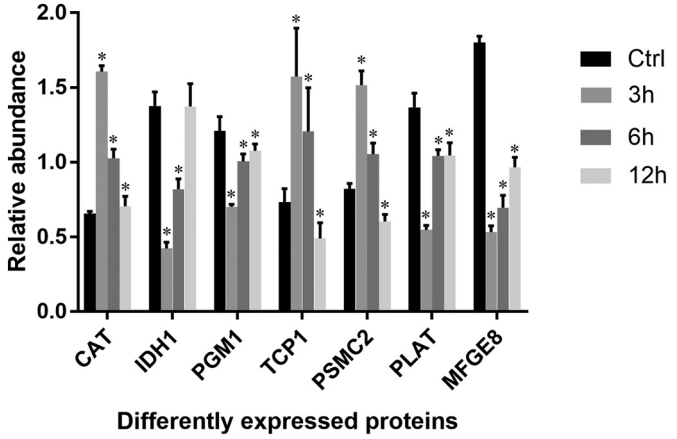

Fig. 7. Verification of the differentially expressed proteins using parallel reaction monitoring (PRM). The relative abundances of the differently expressed proteins from extracellular vesicles (EVs) isolated from PC12 cells subjected to OGD for 0 h (control), 3 h, 6 h, or 12 h, as compared to the EVs of undamaged PC12 cells. The expression of protein was assessed three times. * indicates $p \leq 0.05$ compared with control.

energy generation. We found that IDH1 was downregulated in EVs secreted by OGD-damaged cells, suggesting that the TAC was disrupted in cells subjected to OGD, and that signals of this disruption were transmitted from the damaged donor cells to undamaged recipient cells via EVs (Fig. 7). Thus, our results suggested that the changes in donor-cell carbohydrate metabolism caused by OGD were transmitted to the recipient cells through EVs, disrupting the carbohydrate metabolism of the recipient cells.

Proteins are the ultimate executors of gene function. Thus, the correct translation, folding, and modification of proteins, as well as the timely degradation of misfolded proteins, is required to maintain the stability of the internal cellular environment. Our KEGG pathway analysis showed that, in EVs secreted by cells subjected to short-term OGD (3 h or 6 h), many ribosome pathway proteins were differently expressed (Fig. 5). However, after prolonged OGD (12*h*), ribosome pathway proteins were not differentially expressed between the OGD group and the control (Fig. 5). Instead, many lysosome pathway proteins were differentially expressed in the OGD EVs as compared to the control (Fig. 5). These results suggested that cells responded quickly to OGD, activating a series of signaling pathways and increasing protein synthesis. TCP1, which is an important protein-folding chaperone, cooperates with HSP90 to repair misfolded proteins and to ensure that the translated proteins function normally [29]. We found that TCP1 protein expression levels in the 3 h OGD group were almost twice as high as those of the control group, but that TCP1 expression levels decreased noticeably as OGD duration increased (Fig. 7). In the 12 h OGD group, TCP1 protein expression levels were substantially lower than those of the control group (Fig. 7). As OGD duration increases, the ability of cells to repair misfolded proteins gradually decreases, which leads to accumulation of misfolded protein in cells, eventually inducing apoptosis [30]. Most of the intracellular misfolded proteins are degraded by the proteasome pathway; this degradation process maintains the homeostasis of the intracellular environment [31]. In addition, degraded proteins are used as raw materials for the synthesis of other intracellular substances. Here, PSMC2 proteasome expression was initially upregulated in the EVs in response to OGD, but PSMC2 expression decreased as OGD was prolonged, indicating that the ability of the donor cells to degrade misfolded proteins was depleted over time (Fig. 7). Thus, as OGD duration increased, proteins associated with protein synthesis/repair and degradation were downregulated in the EVs. In addition, KEGG pathway analysis indicated that the accumulation of misfolded proteins further activated the lysosome pathway in the later stages of OGD (Fig. 5). In the EVs derived from damaged cells, the abnormal expression of proteins involved in protein synthesis and degradation altered recipient cell function, and upregulated additional lysosome-associated proteins, leading to the abnormal activation of lysosomes in the recipient cells. Alterations in the expression levels of these proteins in the EVs might be one of the mechanisms that induce recipient cell damage.

IS refers to the formation of a thrombus or embolism, resulting in an insufficient blood supply in local brain tissue, and leading to ischemia and neurocyte hypoxia [1,2]. Thrombolytic therapy is the most effective clinical treatment for IS. Here, several proteins associated with thrombosis were differentially expressed in the EVs derived from the OGD-damaged cells. PLAT, a catalytic enzyme that transforms plasminogen into plasmin, plays a thrombolytic role [32,33]. PLAT was downregulated in the OGD-group EVs as compared to the controls, suggesting the EVs secreted by the OGD-damaged cells aggravated thrombosis (Fig. 7). Serpine1 (PAI1), the most important plasminogen activator inhibitor, significantly inhibits PLAT activity, promoting thrombosis formation [34]. We found that PAI1 expression levels increased in the EVs as OGD duration was prolonged. Simultaneously, the complement system protein was abnormally activated (Fig. 6). Therefore, damaged cell-derived EVs may cross the blood-brain barrier and enter the bloodstream, further promoting the formation of thrombi and aggravating disease development.

Angiogenesis is typically induced in response to ischemic stroke. Our results indicated that MFGE8, which is a key regulator of angiogenesis [35], was strongly downregulated in the EVs secreted by the OGD-damaged cells as compared to the controls (Fig. 7). These results again suggested that EVs derived from OGD-damaged cells might aggravate disease progression.

In addition to the proteins characterized above, several other proteins differentially expressed in the OGD EVs were also associated with the regulation of various signaling pathways related to IS. The proteins differently expressed in the EVs derived from OGD-damaged cells might transmit complicated information through the intact PPI network to the recipient cells. The specific roles and functions of the proteins differently expressed in the EVs derived from OGD-damaged cells remain to be further explored.

5. Conclusions

Our results showed that EVs derived from OGD-damaged cells harmed normal cells, and that the level of harm increased as OGD was prolonged. Using TMT proteomics, we identified and verified several proteins differentially expressed in the OGD EVs. Our proteomic analyses identified a link between proteome alterations and recipient cell death. Thus, EVs secreted by injured nerve cells may aggravate IS by damaging surrounding uninjured cells and promoting thrombogenesis. The seven proteins that we validated might be useful targets for IS diagnosis and treatment. In addition, the proteins identified here deserve further evaluation as potential targets for IS therapy.

Supplementary data to this article can be found online at https://doi.org/10.1016/j.lfs.2019.06.002.

Conflicts of interest

We declare that there are no conflicts of interest.

Acknowledgments

This project was supported by the National Natural Science Foundation of China (Grant number: 81671159 and 31700927).

References

[1] J. Li, S. Zhang, X. Liu, D. Han, J. Xu, Y. Ma, Neuroprotective effects of leonurine against oxygen–glucose deprivation by targeting Cx36/CaMKII in PC12 cells, PLoS

One 13 (2018) e0200705.
[2] S.Y. Park, Y.W. Choi, G. Park, Nrf2-mediated neuroprotection against oxygen-glucose deprivation/reperfusion injury by emodin via AMPK-dependent inhibition of GSK-3b, J. Pharm. Pharmacol. 70 (2018) 525–535.
[3] S.E. Khoshnam, W. Winlow, M. Farzaneh, Y. Farbood, H.F. Moghaddam, Pathogenic mechanisms following ischemic stroke, Neurol. Sci. 38 (2017) 1167–1186.
[4] Z.X. Xu, L. Xu, J.Q. Wang, J. Mang, L. Yang, J.T. He, Expression changes of the notch signaling pathway of PC12 cells after oxygen glucosedeprivation, Int. J. Biol. Macromol. 118 (2018) 1984–1988.
[5] T. Kalogeris, C.P. Baines, M. Krenz, R.J. Korthuis, Ischemia/Reperfusion, Compr. Physiol. 7 (2016) 113–170.
[6] C. Thery, L. Zitvogel, S. Amigorena, EVs: composition, biogenesis and func-tion, Nat. Rev. Immunol. 2 (2002) 569–579.
[7] E.G. Trams, C.J. Lauter, N. Salem Jr., U. Heine, Exfoliation of membrane ecto-enzymes in the form of micro-vesicles, Biochim. Biophys. Acta 645 (1981) 63–70.
[8] H. Tadokoro, T. Umezu, K. Ohyashiki, T. Hirano, J.H. Ohyashiki, EVs derived from hypoxic leukemia cells enhance tube formation in endothelial cells, J. Biol. Chem. 288 (2013) 34343–34351.
[9] N. Osier, V. Motamedi, K. Edwards, A. Puccio, R. Diaz-Arrastia, K. Kenney, J. Gill, EVs in acquired neurological disorders: new insights into pathophysiology and treatment, Mol. Neurobiol. 55 (2018) 9280–9293.
[10] F. Chen, Y. Du, E. Esposito, Y. Liu, S. Guo, X. Wang, E.H. Lo, C. Xing, X. Ji, Effects of focal cerebral ischemia on exosomal versus serum miR126, Transl. Stroke Res. 6 (2015) 478–484.
[11] H. Xin, F. Wang, Y. Li, Q.E. Lu, W.L. Cheung, Y. Zhang, Z.G. Zhang, M. Chopp, Secondary release of EVs from astrocytes contributes to the increase in neural plasticity and improvement of functional recovery after stroke in rats treated with EVs harvested from MicroRNA 133b overexpressing multipotent mesenchymal stromal cells, Cell Transplant. 26 (2017) 243–257.
[12] Doeppner TR, Herz J, Gorgens A, Schlechter J, Ludwig AK, Radtke S, de Miroschedji K, Horn PA, Giebel B, Hermann DM, (2015) Extracellular vesicles improve post-stroke neuroregeneration and prevent postischemic immunosuppression., stem. Cells. Transl. Med. 4 (2015) 1131–1143.
[13] J. Yang, X. Zhang, X. Chen, L. Wang, G. Yang, Exosome mediated delivery of miR-124 promotes neurogenesis after ischemia, Mol. Ther. Nucleic. Acids. 7 (2017) 278–287.
[14] Y. Zhang, M. Chopp, Y. Meng, M. Katakowski, H. Xin, A. Mahmood, Y. Xiong, Effect of EVs derived from multipluripotent mesenchymal stromal cells on functional recovery and neurovascular plasticity in rats after traumatic brain injury, J. Neurosurg. 122 (2015) 856–867.
[15] H.C. Chou, C.H. Lu, Y.C. Su, L.H. Lin, H.I. Yu, H.H. Chuang, Y.T. Tsai, E.C. Liao, Y.S. Wei, Y.T. Yang, Y.A. Chien, X.R. Yu, Y.R. Lee, H.L. Chan, Proteomic analysis of honokiol-induced cytotoxicity in thyroid cancer cells, Life Sci. 207 (2018) 184–204.
[16] D. Luo, S. Zhan, W. Xia, L. Huang, W. Ge, T. Wang, Proteomics study of serum EVs from papillary thyroid cancer patients, Endocr. Relat. Cancer. 25 (2018) 879–891.
[17] C.F. Ruivo, B. Adem, M1. Silva, S.A. Melo, The biology of cancer EVs: insights and new perspectives, Cancer Res. 77 (2017) 6480–6488.
[18] R. Kalluri, The biology and function of EVs in cancer, J. Clin. Invest. 126 (2016) 1208–1215.
[19] G.E. Manuel, T. Johnson, D. Liu, Therapeutic angiogenesis of EVs for IS, Int. J. Physiol. Pathophysiol. Pharmacol. 9 (2017) 188–191.
[20] P. Mathiyalagan, Y. Liang, D. Kim, S. Misener, T. Thorne, C.E. Kamide, E. Klyachko, D.W. Losordo, R.J. Hajjar, S. Sahoo, Angiogenic mechanisms of human CD34+ stem cell EVs in the repair of ischemic hindlimb, Circ. Res. 120 (2017) 1466–1476.
[21] Paul M. Holloway, Felicity N.E. Gavins, Modeling ischemic stroke in vitro: the status quo and future perspectives, Stroke 47 (2016) 561–569.
[22] K.W. Nam, C.K. Kim, T.J. Kim, S.J. An, K. Oh, S.B. Ko, B.W. Yoon, Intravenous thrombolysis in acute IS with active cancer, Biomed. Res. Int. (2017) 4635829, , https://doi.org/10.1155/2017/4635829.
[23] J. Minnerup, H. Wersching, A. Teuber, J. Wellmann, J. Eyding, R2. Weber, G. Reimann, W. Weber, L.U. Krause, T. Kurth, K. Berger, Outcome after thrombectomy and intravenous thrombolysis in patients with acute IS: a prospective observational study, Stroke 47 (2016) 1584–1592.
[24] I. Žitňanová, P. Šiarnik, B. Kollár, M. Chomová, P. Pazderová, L. Andrezálová, M. Ježovičová, K. Koňariková, L. Laubertová, Z. Krivošíková, L. Slezáková, P. Turčáni, Oxidative stress markers and their dynamic changes in patients after acute IS, Oxidative Med. Cell. Longev. (2016) 9761697, , https://doi.org/10.1155/2016/9761697.
[25] S.M. Davis, K.R. Pennypacker, Targeting antioxidant enzyme expression as a therapeutic strategy for IS, Neurochem. Int. 107 (2017) 23–32.
[26] Z. Luo, X. Xu, T. Sho, J. Zhang, W. Xu, J. Yao, J. Xu, ROS-induced autophagy regulates porcine trophectoderm cell apoptosis, proliferation and differentiation, Am. J. Physiol. Cell. Physiol. (2018), https://doi.org/10.1152/ajpcell.00256.2018.
[27] S. Radenkovic, P. Witters, E. Morava, Central nervous involvement is common in PGM1-CDG, Mol. Genet. Metab. 125 (2018) 200–204.
[28] E. Bogdanovic, IDH1, lipid metabolism and cancer: shedding new light on old ideas, Biochim. Biophys. Acta 1850 (2015) 1781–1785.
[29] X.H. Liang, W. Shen, H. Sun, G.A. Kinberger, T.P. Prakash, J.G. Nichols, S.T. Crooke, Hsp90 protein interacts with phosphorothioate oligonucleotides containing hydrophobic 2′-modifications and enhances antisense activity, Nucleic Acids Res. 44 (2016) 3892–3907.
[30] C. Hua, W.N. Ju, H. Jin, X. Sun, G. Zhao, Molecular chaperones and hypoxic-ischemic encephalopathy, Neural Regen. Res. 12 (2017) 153–160.
[31] G.C. Lander, E. Estrin, M.E. Matyskiela, C. Bashore, E. Nogales, A. Martin, Complete subunit architecture of the proteasome regulatory particle, Nature 482 (2012) 186–191.
[32] C. Liang, M. Ding, F. Du, J. Cang, Z. Xue, Tissue plasminogen activator (tPA) attenuates propofol-induced apoptosis in developing hippocampal neurons, Springerplus 5 (2016) 475.
[33] F. Simão, T. Ustunkaya, A.C. Clermont, E.P. Feener, Plasma kallikrein mediates brain hemorrhage and edema caused by tissue plasminogen activator therapy in mice after stroke, Blood 129 (2017) 2280–2290.
[34] S. Peng, G. Xue, L. Gong, C. Fang, J. Chen, C. Yuan, Z. Chen, L. Yao, B. Furie, M. Huang, A long-acting PAI-1 inhibitor reduces thrombus formation, Thromb. Haemost. 117 (2017) 1338–1347.
[35] Akihiko Uchiyama, Kazuya Yamada, Sachiko Ogino, Yoko Yokoyama, Yuko Takeuchi, Mark C. Udey, Osamu Ishikawa, Sei-ichiro Motegi, MFGE8 regulates angiogenesis in cutaneous wound healing, Am. J. Pathol. 184 (2017) 1981–1990.